



**HAL**  
open science

## Sensitivity analysis in a radiological impact assessment of a nuclear power plant discharge. A comparison of the Morris, Spearman and Sobol' approaches

Valerie Nicoulaud Gouin, Christophe Mourlon, Taku Tanaka, Severine Le Dizes-Maurel, Laurent Garcia Sanchez, Jean-Christophe Attard, Benjamin Zorko, Juan-Carlos Mora, Marie Simon Cornu

### ► To cite this version:

Valerie Nicoulaud Gouin, Christophe Mourlon, Taku Tanaka, Severine Le Dizes-Maurel, Laurent Garcia Sanchez, et al.. Sensitivity analysis in a radiological impact assessment of a nuclear power plant discharge. A comparison of the Morris, Spearman and Sobol' approaches. *Journal of Environmental Radioactivity*, 2022, 242, pp.106770. 10.1016/j.jenvrad.2021.106770 . hal-03973081

**HAL Id: hal-03973081**

**<https://hal.science/hal-03973081>**

Submitted on 3 Feb 2023

**HAL** is a multi-disciplinary open access archive for the deposit and dissemination of scientific research documents, whether they are published or not. The documents may come from teaching and research institutions in France or abroad, or from public or private research centers.

L'archive ouverte pluridisciplinaire **HAL**, est destinée au dépôt et à la diffusion de documents scientifiques de niveau recherche, publiés ou non, émanant des établissements d'enseignement et de recherche français ou étrangers, des laboratoires publics ou privés.



Distributed under a Creative Commons Attribution - NonCommercial - NoDerivatives 4.0 International License

# Sensitivity analysis in a radiological impact assessment of a nuclear power plant discharge. A comparison of the Morris, Spearman and Sobol' approaches.

V. Nicoulaud-Gouin<sup>a,\*</sup>, C. Mourlon<sup>b</sup>, T. Tanaka<sup>c</sup>, S. Le Dizes-Maurel<sup>d</sup>, L. Garcia-Sanchez<sup>d</sup>, J.C. Attard<sup>a</sup>, B. Zorko<sup>e</sup>, J. C. Mora<sup>f</sup>, M. Simon-Cornu<sup>g</sup>

<sup>a</sup>*Institut de Radioprotection et de Sûreté Nucléaire, IRSN, PSE-ENV, SRTE, LR2A, Cadarache, France*

<sup>b</sup>*Institut de Radioprotection et de Sûreté Nucléaire, IRSN, PSE-ENV, SEREN, LEREN, Cadarache, France*

<sup>c</sup>*EDF R&D, LNHE, 6 quai Watier, 78400 Chatou, France*

<sup>d</sup>*Institut de Radioprotection et de Sûreté Nucléaire, IRSN, PSE-ENV, SRTE, LR2T, Cadarache, France*

<sup>e</sup>*Jozef Stefan Institute, Jamova cesta, 39, 1000 Ljubljana, Slovenia.*

<sup>f</sup>*UPRPYMA. CIEMAT. Avda. Complutense 40, 28040 Madrid, Spain.*

<sup>g</sup>*Institut de Radioprotection et de Sûreté Nucléaire, IRSN, PSE-ENV, SEREN, Cadarache, France*

---

## Abstract

This paper compares the Morris, Spearman and Sobol' methods of sensitivity analysis in radiological risk assessment. The determination of the most influential parameters on model with regards to the propagation of their uncertainties to output variables, is of greatest interest. This study aims to determine the relative importance of parameters uncertainties on the dose calculation uncertainty in the framework of a scenario of routine discharges discussed in the context of an IAEA working group. The scenario considers atmospheric and liquid discharges of three different types of radionuclides ( $^{14}\text{C}$ , tritium as HTO and  $^{110\text{m}}\text{Ag}$ ) from a nuclear power plant located by the side of a river. It is concluded that the most reliable and practical method according to the ability of ranking influential parameters and the easiness of its application is the Spearman method. As key result, the three first influential variables for annual total dose for all pathways and all radionuclides were the water dissolved inorganic carbon concentration, the volatilisation rate constant and the soil layer solid liquid distribution in  $^{14}\text{C}$ .

*Keywords:* Sensitivity analysis, Morris, Spearman, Sobol', radionuclides, risk assessment

---

## 1. Introduction

Sensitivity analysis aims at ascertaining the relative importance of uncertainties of the different input parameters on the output uncertainty (Saltelli, 2017; Baroni & Tarantola, 2014). This is why sensitivity analysis is intimately linked to uncertainty analysis. No unique definition exists for “sensitivity analysis” as its definition is closely related to its aim, and sensitivity analyses could answer different questions:

For instance it could determine whether a model is in good match of the expecting output: a parameter being exhibited influential by the sensitivity analysis, although it is known as non influential, calls into question the model validity or the knowledge validity of the parameter real impact.

In addition, it could also put in light the interaction between processes considered in the model. Moreover, if it is established that a parameter is not influential, it can be set equal to its deterministic value without distorting the impact on the output.

However the main interest is to identify the most influential parameters on model results to prioritize additional research in order to reduce their uncertainties (Hamby, 1994).

Depending on how these questions are framed and addressed, different types of sensitivity analysis can be distinguished (Pianosi *et al.*, 2016; Borgonovo *et al.*, 2016; Iooss *et al.*, 2015).

The screening method as Morris method, the measures of importance as Spearman or the variance-based global methods as FAST (Fourier Amplitude Sensitivity Testing) (Xue & Gertner, 2011; McRae *et al.*, 1982) or Sobol’ methods are distinguished. Rocquigny *et al.* have proposed decision trees to help the practitioner to choose the most appropriate method for its problem and its model according to the linearity or monotonicity of the model and the CPU time (Rocquigny *et al.*, 2008). Although variational methods such as Sobol’ are more efficient than simple screening methods, their calculation time is often prohibitive. Practitioners prefer to turn to inexpensive methods such as the Spearman or Morris method.

---

\*Corresponding author

*Email address:* `valerie.nicoulaudgouin@irsn.fr` ()

These last two methods can therefore be evaluated against the Sobol' method. A comprehensive evaluation of various sensitivity analysis methods applied to a hydrological model (Gan *et al.*, 2007) shows that Spearman method is inconsistent, Morris method is most efficient but least robust method and Sobol' results are consistent with FAST results. The method of Morris effectively reduces the computational demands of global sensitivity analysis for distributed watershed models (Herman *et al.*, 2013). The meta-model technique is discussed for estimating Sobol' indices at low computational cost, very useful when the physical models under study require prohibitive simulation time for direct calculations. In (Song *et al.*, 2013) first, the Morris screening method was used to qualitatively identify the parameters' sensitivity, and then a few parameters were selected to quantify the sensitivity indices with a variance-based method integrated with a meta-model i.e. Sobol' method integrated with the response surface model. Morris method is therefore used as a qualitative method without being sufficiently efficient to be a quantitative method. In Rivalin *et al.* (2018) Morris method is used to reduce the number of parameters to analyse. In order to perform Sobol' analysis with complex and computationally expensive model, response surfaces are commonly built to approximate these complex models and to allow us the use of variance-based sensitivity methods (Song *et al.*, 2013).

This article focuses on the application of sensitivity analysis to radiological risk assessment: characterization of uncertainties in human exposure pathways and analysis of the impact of these uncertainties on the radioactive contamination is of greatest interest in radiological risk assessment (Hinton *et al.*, 2013; Urso L.*et al.*, 2019). Impact of the uncertainties on radioactive contamination of leafy vegetables in the context of the Fukushima accident was studied by Morris method (Sy *et al.*, 2016). Morris and Sobol' methods were also used for analyzing the sensitivity of parameters of a transfer model describing the contaminated vegetation in the Fukushima prefecture (Nicoulaud-Gouin *et al.*, 2014). The relative influence of uncertain inputs on several outputs from an atmospheric dispersion model applied on the Fukushima nuclear accident was studied by Sobol' indices and Gaussian process emulation (Girard *et al.*, 2016). While studying the environmental, physiological and management

parameters in agroecosystems following an atmospheric radionuclides discharge, Breshears *et al.*, (1992) used Monte-Carlo and full-factorial sampling as a sampling strategy on the PATHWAY model which simulates radionuclide transport through an agroecosystem and conclude on the importance of variance-based sensitivity analysis.

The assessments of radiological impact to people and the environment arising from radionuclides being discharged, were addressed during the IAEA's Modelling and Data for Radiological Impact Assessment (MODARIA) program which ran from 2012 to 2015. In this program the group proposed a scenario of an atmospheric and liquid nuclear power plant discharge. The propagation of different uncertainties in this scenario up to the dose assessment was further discussed in (Mora *et al.*, 2014).

The objectives of this work were to determine the relative importance of parameters uncertainties on the dose calculation uncertainty in the framework of the Modaria scenario; it also aims to determine which of the two methods Spearman and Morris is the most relevant and reliable in this case study.

For these purposes, a variance-based method (Sobol' method) was also involved as a reference method and the Morris and Spearman results were compared according to the capability of discriminating influential from non influential variables, and according to the similarity of ranking the most influential variables.

Sensitivity analysis of input parameters, obtained from the SAMCAT software (Sensitivity Analysis and Markov Chain simulations Applied to Transfer models) (Nicoulaud-Gouin *et al.*, 2016) embedding Morris and Sobol' method and implementing their post-processing, was performed and compared with Spearman method implemented in SYMBIOSE software (Simon-Cornu *et al.*, 2015).

## 2. Materials and Methods

SYMBIOSE is a modelling platform, for predicting the evolution in time and space of the behaviour of radionuclides discharged into watercourses or the atmosphere within the main

environmental compartments, and for assessing the doses and dose rates to which human populations are exposed. Several numerical solvers can be chosen from to resolve differential equations in the different sub-systems of the biosphere (atmospheric, river, agricultural, human).

Table 1 describes the hierarchical interaction matrix between sub-systems of the biosphere in the simulator Biosphere of SYMBIOSE platform.

The adopted scenario with its deterministic and probabilistic inputs will now be detailed. Then the sensitivity analysis methods that we plan to compare in connection with the software implementing these methods (SAMCAT and SYMBIOSE) will be developed in section 2.7. Finally, the tools for comparing these analyses will be set out.

### *2.1. Scenario and landscape*

In the frame of MODARIA Working group 5 (WG5) (Mora *et al.*, 2014), we apply the so-called Chinon scenario using site specific data. WG5 participants were invited to apply their models and/or methodology to study the issue of uncertainties when assessing the impacts of the radioactive routine discharges of a nuclear facility to the environment. The facility considered is the Chinon B site, operated by Electricité De France (EDF), located in France, approximately 40 km South West of the city of Tours. It is composed of four 900 MW Pressurized Water Reactor (PWR) units, hereafter called the Chinon NPP (Figure 1). The participants were invited to perform the Environmental Impact Assessment (EIA) for people living within 5 km of the barycenter of its stacks, considering the liquid and atmospheric discharges of the Chinon NPP over year 2011 (a discharge of mineral and organic  $^{14}\text{C}$ , tritiated water vapour HTO in the atmosphere and a discharge of mineral  $^{14}\text{C}$ , tritiated water vapour HTO and  $^{110\text{m}}\text{Ag}$  in river system). After the discharges, the radionuclides migrate through the river and agricultural systems. In the river system, we set up three river receptor points: the first for drinking water uptake, the second for irrigation, and the third for fishing (Figure 1). The endpoint is the annual effective dose to a representative rural person (ICRP, 2006) living in the location within 5 kilometers of the NPP, where the highest dose was obtained by a pre-calculation. Modelled exposure pathways are external radiation (in the

plume, and outside of the plume), and internal contamination (inhalation, percutaneous transfer for tritium, ingestion of foodstuffs: e.g. drinking water, leafy vegetables, flour, potatoes, cow milk, butter, beef meat, hen eggs, river fish, etc).

Therefore the quantity of interest for this sensitivity analysis is firstly the annual total dose for all pathways. Secondly, two predominant components of this annual dose, the ingestion dose due to  $^3\text{H}$  and  $^{14}\text{C}$ , and two minor components of this dose, the ingestion dose due to  $^{110\text{m}}\text{Ag}$  and the groundshine dose due to  $^{14}\text{C}$ , were considered separately.

The present study focuses specifically on the sensitivity analysis for the scenario.

## *2.2. Used models, deterministic input data and simulations*

Since the total annual dose received by a rural adult population exposed to the Chinon NPP 2011 radioactive discharges is what we are trying to characterize, it is necessary to run the simulations long enough to observe an accumulation in the soil or sediment compartments. On the other hand, probabilistic simulations often take a prohibitive amount of time to compute, so a compromise of three years for each deterministic calculation has been chosen. The 2011 time series for all time depending data (discharges, river data, meteorological data...) were thus reproduced for 2009 and 2010 and the simulation run on the time frame 2009-2011.

Within the SYMBIOSE platform, a specific model, TOCATTA simulates the dynamics of  $^{14}\text{C}$ , HTO and organically bound tritium OBT in agricultural soil and plant ecosystems. This model considers, as source terms, chronical discharges (or accidental releases) of gaseous carbon-14 and tritium into the atmosphere from nuclear facilities and/or the spray irrigation of contaminated water into agricultural soils (Le Dizes *et al.*, 2012).

A deterministic calculation using SYMBIOSE identified the location of the representative person in which he or she receives the highest dose.

Specific deterministic input parameters were introduced in SYMBIOSE and were described in Table 2.

### 2.3. Probability distributions

Table 3 describes different uncertainties of input parameters,  $X_1 - X_{47}$ , that were introduced in the scenario to perform uncertainty analysis and sensitivity analysis with the Spearman and Morris methods. We conducted a Sobol analysis for a group of 12 influential parameters ( $X_{38}, X_{11}, X_3, X_{14}, X_6, X_{44}, X_{43}, X_{16}, X_4, X_7, X_{29}, X_{12}$ ) and 4 non-influential parameters ( $X_5, X_{13}, X_{15}, X_{42}$ ), identified by the Morris method (see results with Figure 2 showing input parameters having a  $\mu^*$  over 0.1) with regards to the total ingestion dose due to  $^{14}\text{C}$ ,  $^{110\text{m}}\text{Ag}$  and  $^3\text{H}$ .

We detail in the appendix the probability distribution for each sub-system of the biosphere (ie each cell in the diagonal of Table 1), except "Discharges" and "Atmospheric system" for which no parameteric uncertainty was considered.

### 2.4. Spearman method

The commonly used method of Spearman correlation  $\rho$  is well described in the literature (Spearman, 1904; Gibbons & Chakraborti, 1992). The Spearman correlation coefficient is defined as the Pearson correlation coefficient between the rank variables:

$$\rho(r_{gX}, r_{gY}) = \frac{\text{cov}(r_{gX}, r_{gY})}{\sigma_{r_{gX}} \sigma_{r_{gY}}} \quad (1)$$

where  $r_{gX}$  and  $r_{gY}$  are the ranks variables of the variables X and Y respectively,  $\text{cov}(r_{gX}, r_{gY})$  is the covariance of the rank variables, and  $\sigma_{r_{gX}}$  and  $\sigma_{r_{gY}}$  are the standard deviations of the rank variables.

The rank transformation of data is used to overcome the poorly performing of Pearson correlation when the relationships between input factors and the model output are non-linear. However this method is reliable in the case of monotonic relationships.

The Latin Hypercube Sampling (LHS) was used to optimize the number of simulations to be performed and also to ensure that the sampling can cover a parametric domain close to the theoretical distribution. However, this method can introduce undesirable correlations

between parameters in small samples (Harris, 1995). And the coverage of space is not complete. But we checked that the number of non-wanted correlations in the LHS was low and did not interfere with the results.

Test of significance of the Spearman coefficients, based on  $\chi^2$  statistics provides a probability called P-value indicating whether the correlation is significant or not (Fieller *et al.*, 1957; Choi, 1977). If the P-value is small, we reject the idea that the correlation is due to random sampling. If the P-value is large, the data give no reason to conclude that the correlation is real. This is not the same as saying that there is no correlation at all. There is just no clear evidence that the correlation is real or not from a fortuitous consequence.

Confidence intervals of the Spearman coefficients could be calculated by using the Fisher transformation (Fieller *et al.*, 1957; Choi, 1977).

### 2.5. Morris method

The screening method developed by Morris (Morris, 1991), and also known as elementary effects method, was used, thanks to SAMCAT software. It relied on 960 simulations (20 repetitions of the initial and one-at-a-time (OAT) Morris design of 4 levels with the 47 input parameters). The advantages of using Morris method are the low computational cost and its independence with regards to non-linearity or non monotonicity of the model. Two sensitive measures  $\mu$  and  $\sigma$  are associated to each parameter, both based on the calculation of incremental ratios ( $R_i^k$ ) at various points of the input hypercube space, spaced by a fixed step  $\frac{1}{l-1}$  where  $l$  is a selected level and known as “elementary effects”. The mean of all the ratios  $\mu$  assessing the overall influence of the parameter on the output and their standard deviation  $\sigma$  estimating the totality of the higher-order effects, are calculated over  $r$  different trajectories. The cost of the method is  $r \times (p + 1)$ , if  $p$  is the number of parameters. Briefly, the sampling strategy for the Morris method is to generate a lot of different trajectories in the parametric space (random starting point and then moving one factor at a time in random order). And then it chooses the best (with the highest spread)  $r$  of them for actual

model runs. For the parameter  $X_i$  with  $r$  trajectories, we have:

$$R_i^k = \frac{f(X_1, \dots, X_{i-1}, X_i + \Delta_i^k, X_{i+1}, \dots, X_p) - f(X_1, \dots, X_i, \dots, X_p)}{\Delta_i^k} \quad (2)$$

$$\Delta_i^k \in \left\{ \frac{1}{l-1}, \frac{2}{l-1}, \dots, 1 - \frac{1}{l-1} \right\} \quad (3)$$

$$\mu_i = \frac{1}{r} \sum_{k=1}^r R_i^k \quad (4)$$

$$\sigma_i = \sqrt{\frac{1}{r-1} \sum_{k=1}^r (R_i^k - \mu_i)^2} \quad (5)$$

$$\mu_i^* = \frac{1}{r} \sum_{k=1}^r |R_i^k| \quad (6)$$

A large value of  $\mu_i$  underlines a relatively influential parameter. A large value of  $\sigma_i$  underlines that the elementary effects are enough different. That is due to a non-linear response with regards to the parameter  $X_i$  or to the fact of an interaction with other parameters. This estimation of the only combined effects is a disadvantage of this method. When  $\mu_i$  is near zero, we can have weak elementary effects or a compensation of negative and positive effects. To remove this ambiguity in the interpretation of a weak  $\mu_i$ , the absolute value of the ratios  $\mu_i^*$  was taken.

As suggested by (Campolongo *et al.*, 2007), the level  $l$  is preferentially even and  $r$  is in general between 10 and 50.

A diagram  $\sigma$  over  $\mu^*$  visualizes the influence of each parameter (see Figure 2 for example).

Confidence intervals can be assessed for each indices  $\mu^*$  et  $\sigma$ . The confidence intervals are bilateral with a  $1 - \alpha$  probability and the student law  $T$  is used for the indices  $\mu_i^*$  and the  $\chi^2$  law for the indices  $\sigma_i$ .

$$IC_{\mu_i^*} = \mu_i^* \pm \frac{T_{r-1}(1 - \alpha/2)\sigma_{\mu_i^*}}{\sqrt{r}} \quad (7)$$

$$IC_{\sigma_i^*} = \left[ \sqrt{\frac{(r-1)}{\chi^2(r-1, \alpha/2)}} \sigma_i, \sqrt{\frac{(r-1)}{\chi^2(r-1, 1 - \alpha/2)}} \sigma_i \right] \quad (8)$$

## 2.6. Sobol' method

The purpose of being able to quantify the contribution of inputs to the variance in the selected output, is a key focus of global sensitivity analysis and Sobol' method provides these quantitative measures (Saltelli *et al.*, 2000). It is a variance-based method assuming that the model parameters are independent or uncorrelated. The main advantage in variance-based methods is that they are independent from linearity and monotonicity of the input-output mapping. The total variance of the model output is decomposed with the variance from each individual parameters, and cooperative parameters. That means:

$$V(y) = \sum_{i=1}^p (V_i + \sum_{i \leq j \leq p} V_{ij} + \dots + V_{1\dots p}) \quad (9)$$

$V_i$  denotes the first order contribution of the  $i$ th model parameter,  $V_{ij}$  denotes the pairwise interactive effect of the  $i$ th and  $j$ th parameters. The first order Sobol' index and the total order Sobol' index are expressed by:

$$S_i = \frac{V_i}{V(y)} \quad (10)$$

$$S_{T_i} = 1 - \frac{V_{-i}}{V(y)} \quad (11)$$

where  $V_{-i}$  denotes the contribution of all except the  $i$ th parameter. Therefore compared to Morris or Spearman method it calculates both first and total order effects although it is computationally expensive and not feasible for a lots of input parameters. (Saltelli, 2002) proposed an extended method which the cost is  $10\,000 \times (2p+2)$  model evaluations. However this cost is too important for the SYMBIOSE code with regards to the simulation time of each model evaluation even if we reduce the number of studied parameters. Therefore a technique to overcome this difficulty is called by building a neural network imitating the original code. It is well known as a response surface or meta-model. It used a weighted activation function of the input parameters.

For ensuring the validity of this procedure, the neural network was built on a basis sample

and a test sample was used to test if a well-adapted response surface was obtained. Two measures of accuracy were used to ensure the validity of the surrogate model:

Geometric Reliability Index (GRI) is a dissimilarity measure, quantifying the accuracy factor of predictions around observed values. It is defined by (Jachner *et al.*, 2007):

$$GRI = \frac{1 + \sqrt{\frac{1}{n} \sum_i \left( \frac{\hat{y}_i - y_i}{\hat{y}_i + y_i} \right)^2}}{1 - \sqrt{\frac{1}{n} \sum_i \left( \frac{\hat{y}_i - y_i}{\hat{y}_i + y_i} \right)^2}} \quad (12)$$

and optimal values correspond to 1. The efficiency factor EF (Nash & Sutcliffe, 1970) is a validation measure, ranging from  $-\infty$  to 1:

$$EF = 1 - \frac{\sum_i (\hat{y}_i - y_i)^2}{\sum_i (\hat{y}_i - \bar{y})^2} \quad (13)$$

where prediction power increases as EF tends to ideal value 1, corresponding to exact model predictions.

For conducting reliable Sobol' sensitivity analysis, a low discrepancy input sample was generated by the Sobol' sequences (Bratley & Fox, 1988) combined with a quasi-Monte Carlo sample. the independance of the input variables was also checked.

Confidence intervals of Sobol' indices were also calculated by applying 1000 bootstrap sampling (Saltelli, 2002).

### *2.7. Methodology and implemented software: The graphical user interface SAMCAT*

The procedures adopted to apply these methods and the implementation of the SAMCAT software are given below.

We conducted a Morris analysis with 960 simulations (20 repetitions of the initial Morris design of 4 levels with the 47 input parameters) and a Spearman analysis with a 1000 Latin Hypercube Sampling. Fortunately with 1000 iterations, we obtained less than 0.1

correlations between input parameters in this Spearman sampling which is quite acceptable for conducting a sensitivity analysis.

A cost ( $1000 \times (2p+2)$  or even  $1000 \times p$  let 96000 or 47000 with all parameters) is too expensive computational cost for Symbiose Software. Therefore, we have to build a meta-model with a reduced number of parameters. We choose the most influential parameters for the Morris method and add few other being not influential and calculate Sobol' indices for these parameters with the metamodel: We conducted a Sobol analysis for a group of 12 influential parameters ( $X_{38}, X_{11}, X_3, X_{14}, X_6, X_{44}, X_{43}, X_{16}, X_4, X_7, X_{29}, X_{12}$ ) and 4 non-influential parameters ( $X_5, X_{13}, X_{15}, X_{42}$ ), identified by the Morris method (see on Figure 2 input parameters having a  $\mu^*$  over 0.1) concerning the total ingestion dose in  $^{14}\text{C}$ , in  $^{110\text{m}}\text{Ag}$  and in  $^3\text{H}$ . Two sets of 1000 sampling were launched on Symbiose, one was used for building neural networks and the other for testing the validity of a meta-model constructed. Goodness-of-fit on test basis were gathered in the Table 4 showing a good adequation for using these neural networks in Sobol' analysis which requires  $(16 + 2) \times 10000 = 180\,000$  simulations.

All Morris and Sobol' simulations were configured and analyzed with the SAMCAT software ("Sensitivity Analysis and Markov Chain simulations Applied to Transfer models") (Nicoulaud-Gouin *et al.*, 2016). SAMCAT greatly assists the user in the management and interpretation of sensitivity analysis. It consists of a graphical user interface, developed under the R environment (R Development Core Team, 2012), that automatically prepares input samples, involves Morris or Sobol' methods with the Sensitivity R package (Pujol, 2016), dialogues with SYMBIOSE, implements graphical output and records all the plots in the R expression as bitmap images, then inserts them into an HTML page and finally creates an animation using the SciAnimator library (Xie, 2011). The RNNS software (Bergmeir & Benetez, 2012) wrapping the SNNS (Zell *et al.*, 1998) simulator to make it available from within R was used to build the neural networks for the different studied outputs.

## 2.8. Factors classification

Thresholds for assessment of important factors were chosen according to previous studies (Sin *et al.*, 2011). In particular, threshold value of 0.1 was used for the absolute value of  $\rho_i$  and for  $\mu_i^*$  whereas 0.01 was used for  $S_i$ . Choice of threshold value of 0.01 for  $S_i$  is related to the fact that for a linear model  $S_i = \rho_i^2$ . All factors having  $\mu_i^*$  lower than 0.1 have been considered non- influential for Morris screening application.

We made comparison between different sensitivity methods by considering most reliable method (Sobol') as reference method (Cosenza *et al.*, 2013), with following approaches:

- Scatter plots between  $S_i$  and  $\rho_i$  and between  $S_{T_i}$  and  $\mu_i$  denotes the similarity of sensitivity indices compared to the reference method (factors prioritisation);
- A similarity of ranking of sensitivity indices was compared to the reference method (associated to a factors prioritisation); Modified position factor (PF) was related to the comparison of the position ranking order obtained for the n factors by applying two different methods (i and j) is defined as (Ruano *et al.*, 2012):

$$PF = \sum_{k=1}^p \frac{|P_{k,i} - P_{k,j}|}{\mu_{P_{k,i}, P_{k,j}}} \quad (14)$$

where  $P_{k,i}$  and  $P_{k,j}$  respectively represent the position of the k-th factor in the ranking obtained by applying method i and j respectively and  $\mu_{P_{k,i}, P_{k,j}}$  is the average of  $P_{k,i}$  and  $P_{k,j}$ .

PF is null in case the ranking of all factors is the same. PF is maximum in case the ranking of all factors is completely different for the two different methods.

- similarity of classification into important/non-influential factors compared to the reference method (factors prioritisation and factors fixing);

### 3. Results and discussion

The order of magnitude of the mean (and median) estimated annual total dose is 0.47  $\mu$  Sv. Uncertainty can be quantified by a 95 % confidence interval of [0.37; 0.60]. Roughly, slightly more than a half is due to  $^3\text{H}$ , slightly less than half is due to  $^{14}\text{C}$ , and few percents are due to  $^{110\text{m}}\text{Ag}$ . The ingestion pathway represents a very dominant contribution to the total dose, mainly due to the ingestion of vegetables, river fish and water. The objective of this article is not to detail further these results, but to focus on sensitivity analysis.

#### 3.1. All pathways

According to the Sobol' method, the most influential parameters for the annual total dose for all pathways and all radionuclides were the following ones in decreasing order (Table 6):

- $X_{14}$  the water dissolved inorganic carbon concentration,
- $X_{44}$  the volatilisation rate constant,
- $X_{43}$  the soil layer solid liquid distribution in  $^{14}\text{C}$ ,
- $X_{11}$  the dry matter fraction in fruit vegetable,
- $X_{38}$  the respiratory recycling index in fruit vegetable,
- $X_{29}$  the vegetable isotopic discrimination,
- $X_6$  the fish water content,
- $X_3$  the plant daily irrigation rate in fruit vegetable,
- $X_7$  the reference coefficient partition in suspended matter for Ag,
- $X_{16}$  the water infiltration rate

The two other methods (Morris and Spearman) identified the same influential parameters except for the reference coefficient partition in suspended matter ( $X_7$ ) which did not appear as influential according to Spearman method with a correlation coefficient of 0.065

inferior to 10%. The agreement of the most influential variables between the three methods suggests that applying Sobol' to all potentially influential variables from the Morris study is justifiable. The rankings between these most influential parameters were close between Sobol's and Spearman methods but they were very different between Sobol's and Morris methods. Ranking for Morris method were  $X_{38}$ ,  $X_{11}$ ,  $X_3$ ,  $X_{14}$ ,  $X_{29}$ ,  $X_6$ ,  $X_{44}$ ,  $X_{43}$ ,  $X_{16}$ . denoting a different behaviour in the analysis of the sensitivity between the two methods. Now we are focussing on the different pathways and radionuclides in analysing the ingestion dose due to each radionuclides and the groundshine due to  $^{14}\text{C}$  for a better understanding of the differences in sensitivity assessment.

### 3.2. Ingestion dose due to $^{110\text{m}}\text{Ag}$

The main difference between Spearman method and the two other methods was the ranking of the two or three most influential parameters (see plot at the top left of the figures Figure 2, 3, 4 ):

- The reference coefficient partition in suspended matter ( $X_7$ ) had a Spearman coefficient  $\rho$  of 0,48 [0,43;0,53]. Its Morris indices were  $\mu^* = 0.37$  ([0.26;0.48]) and  $\sigma = 0.23$  ([0.18;0.34]), and its Sobol' indices were  $S = 0.317$  ([0.29; 0.33]),  $T = 0.32$  ([0.30; 0.33]);  $X_7$  is strongly influential for Sobol' and Spearman method whereas it is averagely influential for Morris method. That is due to the fact that the high values of  $X_7$  were not well represented by the Sobol' or Spearman sample,  $X_7$  having a log normal distribution, whereas Morris sample took into account these high values.
- The plant daily irrigation rate in leafy vegetable ( $X_4$ ) had a Spearman coefficient  $\rho$  of -0,15 ([-0,21;-0,09]). Its Morris indices were  $\mu^* = 1.13$  ([0.83;1.43]) and  $\sigma = 1.24$  ([0.94;1.82]), and its Sobol' indices were  $S = 0.62$  ([0.59; 0.65]),  $T = 0.63$  ([0.61; 0.64]);  $X_4$  is also strongly influential for Sobol' and Morris method and very moderately influential for Spearman method.
- The plant daily irrigation rate in fruit vegetable ( $X_3$ ) had a Spearman coefficient  $\rho$  of 0.05 with a p-value of 0.13 ([-0,015;0,11]). Its Morris indices were  $\mu^* = 0.27$

([0.16;0.38]) and  $\sigma = 0.36$  ([0.27;0.52]), and its Sobol' indices were  $S = 0.04$  ([0.03; 0.045]),  $T = 0.04$  ([0.03; 0.05]);  $X_3$  is averagely influential for Morris method, very weakly influential for Sobol' method and not influential for Spearman method.

### 3.3. Ingestion dose due to $^3\text{H}$

The three methods agreed to elect the isotopic discrimination in fruit vegetable ( $X_{29}$ ) as the most influential parameter on the ingestion dose due to  $^3\text{H}$  (see plot at the top right of the figures Figure 2, 3, 4 ). The impact of this parameter seems strong and could be due to the range of uncertainty taken for this parameter ([0.77;1.28] in Table 3). In literature the mean value of isotopic discrimination factor was from 0.46 to 0.72 (Davis *et al.*, 2002; Kim & Baumgartner, 1994), which are less than minimum of triangular distribution taken for this parameter. However this distribution could be justified by the fact that an isotopic dilution of non exchangeable organic bound tritium (neOBT) took place by the rinsing of dry matter. This is why a correction factor has to be applied in order to take into account this phenomena (Le Goff *et al.*, 2014). Previous article (Renard *et al.*, 2017) found that there is no measurable discrimination of tritium in the plant organic matter produced by photosynthesis in ryegrass. It suggests that the disparity in the literature of the OBT/TFWT ratios at the point where equilibrium is attained, (varying from 0.55 to 2.88 depending on the source) could be due to a failure to factor in initial activity of the seed or an inadequate control of tritium activity in the laboratory environment during the rehydration of freeze-dried samples (tritium atmosphere in the water vapour of the laboratory air is not equal to the tritium activity during plant growth). Indeed at the beginning of its development, the plant will produce its first leaves and roots not by photosynthesis but by translocation of matter from the seed. So concretely at the level of the leaves for example, a part of the dry matter comes from the matter produced by photosynthesis (thus must be associated with the tritiated activity during the culture) and another part comes from the seed (thus associated with the tritiated activity of the seed).

However, this study is limited to ryegrass and in order to confirm a isotopic discrimination close to 1, several other plant species as wheat or lettuce have to be studied.

Two other parameters (the dry matter fraction in fruit  $X_{11}$  and leafy  $X_{12}$  vegetable) were less important for the three methods.

### 3.4. Ingestion dose due to $^{14}\text{C}$

#### 3.4.1. Volatilisation

The volatilisation rate constant ( $X_{44}$ ) can influence the ingestion dose by playing a key role in the carbon cycle between soil and plant.

Because of the carbon cycle between the soil and the plant, the volatilization loss from the labile pool becomes a gain to the organic pool through the plant via the plant residues in the litter.

This parameter is influential for each methods but the level of influence is quite different for the Spearman and Sobol' methods on one hand and for the Morris methods on the other hand.

We find a strong influence of this parameter with a Spearman coefficient of 0.45 (confidence interval [0.40, 0.50]) and a first Sobol' index of 0.21 (confidence interval [0.14, 0.26]) whereas the influence is smaller with a Morris index  $\mu^*$  of 0.12 (confidence interval [0.06, 0.18]) and a standard deviation of 0.12 (confidence interval [0.09, 0.18]).

The distribution law form is obviously the cause of this phenomena.

#### 3.4.2. Water infiltration rate

Regarding the water infiltration rate ( $X_{16} = v_s^{Infil}$ ), its implication in ingestion dose is also due to the volatilisation flux  $T^{mig}$  which is nourished by the labile concentration carrying notably the migration flux  $\lambda^{mig}$  (eq 15), 16).

$$\lambda^{mig} = \frac{v_s^{Infil}}{h_p * (\theta + \rho_b * K_d)} \quad (15)$$

$$T^{mig} = \lambda^{mig} * K_h * R_{gas} * T_s * C_{labile} \quad (16)$$

Equation 15 indicates also the possible implication of the variables  $\theta$  ( $X_{17}$ ),  $\rho_b$  ( $X_{18}$ ) and  $K_d$  ( $X_{43}$ ) in the ingestion dose. The relatively weak Spearman coefficient of -0.09 (with a

confidence interval of [-0,15;-0,03]) is in relation with the very weak morris indices ( $\mu^* = 0.1$  [0.06;0.16],  $\sigma = 0.10$  [0.08;0.15]) and a first Sobol' index of 0.01 (with a confidence interval of [0.003;0.03]).

### 3.4.3. Reference coefficient partition

The influence of reference coefficient partition in  $^{14}\text{C}$  ( $X_{43}$ ) is quite different for the Spearman method on one hand and for the Morris and Sobol' methods on the other hand. Its behaviour is alike the volatilisation rate constant. At the end of the simulation, we denote a quite average influence of this parameter with a Spearman coefficient of 0.28 (with a confidence interval of [0,22;0,34]) whereas it is largely less influential with a Morris index  $\mu^*$  of 0.11 (with a confidence interval of [0.03;0.18]) with a standard deviation  $\sigma$  of 0.16 (with a confidence interval of [0.12;0.24]) and a first Sobol' index of 0.08 (with a confidence interval of [0.04;0.12]). The Morris plot (Figure 2) does not denote a non-monotony of the model implying these two parameters as the standard deviation  $\sigma$  has the same magnitude than the mean  $\mu^*$ . The difference of results between Spearman and Morris and Sobol' method is certainly due to the interaction between input parameters since the variable  $X_{43}$  is on the diagonal of the Morris plot.

### 3.4.4. Daily irrigation rate

The daily irrigation rate in fruit vegetable ( $X_3$ ) is the second last influential variable in the Sobol' plot (Figure 4) with a first Sobol' index of 0.03 (with a confidence interval of [0.009;0.06]). With Morris plot (Figure 2), it is the third influential variable ( $\mu^* = 0.26$  [0.17;0.33],  $\sigma = 0.17$  [0.13;0.24]) whereas it is the least influential variable in the Spearman tornado chart (Figure 3) with a Spearman coefficient of 0.14 (with a confidence interval of [0,08;0,20]).

The fact that the variable "daily irrigation rate" is non influential for annual crops whereas it is influential for fruit vegetables can be explained by the fact that the irrigation interception coefficient for annual crop is twice the one for vegetable crop. Consequently the flux of wet input in annual crop soil is less than in vegetable crop soil.

#### 3.4.5. Respiratory recycling index

The respiratory recycling index in fruit vegetable ( $X_{38}$ ) is the most influential parameter for the Morris ( $\mu^* = 0.49$  [0.32;0.67],  $\sigma = 0.40$  [0.26;0.52]) while it is only the sixth influential parameter for the Spearman method ( $\rho = 0.21$  with a confidence interval of [0,14;0,27]) and it is averagely influential for Sobol' method ( $S = 0.07$  [0.03;0.11]). Intimately linked to volatilized activity, it is referred to the respiratory flux of  $CO_2$  fixed by the photosynthesis with regards to the total respiratory flux (Greaver *et al.*, 2005). The probability distribution was established by the Bioprota international group (Limer *et al.*, 2012). It remains a strong influential parameter and the range of its value is always an ongoing research. We have to note that the respiratory recycling index in annual crop ( $X_{37}$ ) is not influential in the ingestion dose due to  $^{14}C$  although the range of its uncertainty is larger than the uncertainty of the respiratory recycling index in vegetable (the uncertainty expanse of  $X_{37}$  is 0.38 whereas the uncertainty expanse of  $X_{38}$  is 0.26). Indeed, the respiratory recycling index nourishes the organic matter concentration via the volatilisation flux and more precisely the litterfall flux. However for annual crop the litterfall is nil between the date of the last harvest and the next germination, unlike to the vegetable crop. Therefore the impact of  $X_{37}$  uncertainty vanishes with regards to the impact of  $X_{38}$  uncertainty because during between 35 days (for root and tuber crop) and 161 days (for animal spring cereal) by year no litterfall occurred onto annual crop soil.

#### 3.4.6. Dissolved Inorganic carbon concentration

For the dissolved inorganic carbon concentration [ $C_{12}^{river}$ ] ( $X_{14}$ ), the results were quite different between the Spearman method with a high negative Spearman coefficient  $\rho$  of -0,65 ([-0,68;-0,61]) and the Sobol' indices  $S = 0.26$  ([0.21; 0.31]),  $T = 0.26$  ([0.21; 0.31]) in one hand and the moderately strong Morris indices  $\mu^* = 0.24$  ([0.17; 0.30]),  $\sigma = 0.13$  ([0.10;0.20]), in the other hand. The dissolved inorganic carbon concentration is involved in the equation giving the dynamic of the fresh fish concentration in  $^{14}C$  ( $[C_{14}^{FreshFish}]$  in eq. 17). Through this equation, the strong impact of its uncertainty compared to the fish

water content uncertainty impact ( $\theta_{fish}$  or  $X_6$ ) or the phytoplankton stable carbon concentration uncertainty impact ( $[C_{12}^{phyto}]$  or  $X_{22}$ ) is understandable.

$$\frac{\partial[C_{14}^{FreshFish}]}{\partial t} = (1 - 1000 \times \theta_{fish}) \times \frac{[C_{12}^{phyto}]}{[C_{12}^{river}]} \times [C_{14}^{river}] \times \lambda^{bio}(1 - \lambda^{bio}e^{-\lambda^{bio}t}) \quad (17)$$

where  $\lambda^{bio}$  is the biological renewal rate of  $^{14}\text{C}$  in the fish, and  $[C_{14}^{river}]$  is the total (water and matter in suspension) concentration of  $^{14}\text{C}$  in the river.

However, this strong impact on the total ingestion dose uncertainty could be reduced if the model takes into account the loss by diffusion or volatilisation of  $^{14}\text{C}$  between the water and the atmosphere.

#### 3.4.7. Fish water content

For the fish water content  $\theta_{fish}$  ( $X_6$ ), the results were quite different between the Spearman method with a relatively strong negative Spearman coefficient  $\rho$  of -0,27 ([-0,33;-0,21]) in one hand and the weak Morris indices  $\mu^* = 0.13$  ([0.11;0.15]),  $\sigma = 0.04$ ([0.03;0.05]), and the very weak Sobol' indices  $S = 0.06$  ([0.03;0.08]),  $T = 0.06$  ([0.03; 0.08]) in the other hand.

Given the equation 17 the uncertainty of phytoplankton stable carbon concentration ( $[C_{12}^{phyto}]$ ) varying from 0.436 to 0.564 and the uncertainty of the term  $(1 - 1000 \times \theta_{fish})$  varying from 0.15 to 0.272, the relative importance of the  $[C_{12}^{phyto}]$  uncertainty would be more important than the fish water content uncertainty.

#### 3.4.8. Dry matter content

For the dry matter content in fruit vegetable ( $X_{11}$ ), the results were similar for the three methods:

- it is the third most influential parameter with the Spearman method, with a relatively strong Spearman coefficient  $\rho$  of 0,29 ([0,24;0,35]),

- it is the second most influential parameter with the Morris method, with indices  $\mu^* = 0.38$  ([0.27;0.50]),  $\sigma = 0.25$  ([0.19;0.37]),
- it is the third most influential parameter with the Sobol' method, with indices  $S = 0.08$  ([0.04;0.12]),  $T = 0.13$  ([0.08; 0.19]).

We also denoted with the three methods a very weak sensitivity of the dry matter content in leafy vegetable and root vegetable, whereas the uncertainties of these three parameters were similar. It was certainly due to the fact that the growth rate in fruit vegetable ( $0.0005 \text{ kg.m}^{-2}.\text{d}^{-1}$ ), by which the harvestable yield is calculated over the vegetative period,

was ten times less important than in leafy or root vegetable ( $0.005 \text{ kg.m}^{-2}.\text{d}^{-1}$ ). Therefore the dilution by the biological growth induced more loss of  $^{14}\text{C}$  in leafy or root vegetable and the impact of the dry matter content follows this dilution phenomena.

### 3.5. Groundshine dose due to $^{14}\text{C}$

The groundshine dose is due to the concentration of  $^{14}\text{C}$  in soil root layer composed by a organic pool where notably the dry soil bulk density and the clay plus silt fraction are involved. The soil layer is also composed by a labile pool where the migration, respiratory and volatilisation processes are involved. Therefore, the parameters and processes described above can influence the groundshine dose.

#### 3.5.1. Dry soil bulk density

The dry soil bulk density ( $X_{18}$ ) shows a negative influence on the external dose since the Spearman coefficient is -0.22 (confidence interval [-0,28, -0,16]) and appears highly influential with the Morris method ( $\mu^* = 0.32$  [0.17;0.46],  $\sigma = 0.31$  [0.23;0.46]).

The USDA-NRCS (USDA, 2008) provides rough guidelines for the minimum dry bulk density at which root growth is affected for various soil textures. The ideal bulk density is lower than  $1.6 \text{ g/cm}^3$  for a sands, loamy sands, with a marginal bulk density of  $1.69 \text{ g/cm}^3$  and a root restricting bulk density up to  $1.80 \text{ g/cm}^3$ . Therefore in order to reduce the influence of this parameter it would be interesting to know the true uncertainty of soil bulk

density which could be lower than  $1.8 \text{ g/cm}^3$ . Agricultural practices (as tillage and heavy equipment) compact soil below the ploughing layer of soil, preventing root penetration and water movement through the soil profile (Weil & Brady, 2016).

There is a relationship between the total porosity  $f_t$  and the dry soil bulk density : if  $\rho_b$  is the bulk density and  $\rho_s$  is the particles density supposed by simplification equals to  $2.65 \text{ g/cm}^3$ ,

$$f_t = \left(1 - \frac{\rho_b}{\rho_s}\right) \quad (18)$$

The deterministic value of the porosity  $pe_{\text{ymbiose}}$  is close to the total porosity obtained with the deterministic value of the bulk density for a sandy soil:

$$f_t = \left(1 - \frac{\rho_b}{\rho_s}\right) = \left(1 - \frac{1.55}{2.65}\right) = 0.41 \quad (19)$$

$$pe_{\text{ymbiose}} = 0.475 \quad (20)$$

The effective porosity is linked to the saturated water content by this relation :if  $\theta_s$  is the saturated water content and  $\theta_r$  the residual water content,

$$p_e = \theta_s - \theta_r \quad (21)$$

Therefore, the porosity and the water content are negatively highly correlated to the dry soil bulk density and we will expect a high influence of these two parameters on the ground-shine dose. However the sensitivity methods presented in this study, could not recognize the influence of the correlated variables because by construction the variables in the sample of Spearman or Morris and even of Sobol', are totally independant. The unique information given by these methods is the direct influence of the variable. Although the porosity and the water content do not have direct influence on the external dose, we cannot know whether there is a direct or indirect influence due to the natural correlation of these variables.

### 3.5.2. Difference between sensitivity analysis methods

All the influential parameters for the groundshine dose due to  $^{14}\text{C}$  were also influential for the ingestion dose due to  $^{14}\text{C}$  (Table 8, and Figures 2, 3, 4) and the same results with regard to the difference of ranking between Spearman and Morris and Sobol' methods were observed. Table 5 traces the position factor  $PF$  between the Morris and Sobol' method on the first hand and between the Spearman and Sobol' method on the other hand. The worst case for eight variables would be 7.11 therefore the best fit between methods is expressed by the Spearman method. The same observation can be done with the scatter plot between Sobol' indices and Morris indices and the scatter plot between Sobol' indices and Spearman coefficients (Figure 6).

Table 7 shows the differences between Morris indices and Spearman coefficients results for the ingestion dose due to  $^{14}\text{C}$ . These results can also be compared with the Sobol' total indices in Table 8. The four first parameters are the same for the Spearman and Sobol' methods. After there is a ranking inversion between the  $X_{38}$  and the  $X_6$  parameters and the two following ones ( $X_3$  and  $X_{16}$ ) are the same. On the other hand the ranking with Morris method is very different from the one with Sobol'. In particular, the parameter  $X_{38}$  placed in 4th position with Sobol' method is the most influential parameter with the Morris method. While the most influential parameter of the Sobol' method  $X_{14}$  is found in 4th position with the Morris method.  $X_3$  is placed in 3rd position with Morris and in 7th position with Spearman or Sobol'. In the same way  $X_{44}$  is in sixth position with Morris and in second position with Spearman or Sobol'.

### 3.6. Interactions impact

We can also note the need for variance-based methods to properly analyze the sensitivities of each parameter. Indeed, the total Sobol' indices for some significant parameters ( $X_{44}$ ,  $X_{43}$ ,  $X_{11}$ ,  $X_{38}$ ) are sufficiently larger than the first order indices. This indicates a non-additive behavior of the model and a possible non-monotonicity of the model.

The contribution of the interaction between input parameters is represented by the difference between Sobol' total and first indices (Figure 5) in which the volatilisation rate constant

( $X_{44}$ ) has the highest average Sobol' interaction contribution of 0.11. It can explain the difference of behaviour of Sobol' total index (0.32 with confidence interval of [0.26;0.38]) compared to its Morris indices ( $\mu^* = 0.12$  [0.06;0.18] and  $\sigma = 0.12$  [0.10;0.19]). The Spearman coefficient (0.45 with a confidence interval of [0.39;0.49]) were similar to the Sobol' results. The distribution coefficient in  $^{14}\text{C}$  ( $X_{43}$ ) has also an average Sobol' interaction contribution of 0.06. The phenomena of volatilisation being close to what is happening in soil system. These two parameters  $X_{43}$  and  $X_{44}$  could certainly interacted amongst themselves.

This dotchart also shows the interaction contributions of the parameters of plant daily irrigation rate ( $X_3$  with 0.035) and the dry matter content  $f^S$  in fruit vegetable ( $X_{11}$  with 0.086) . The contributions could result from the equation associating those parameters with the irrigation captation factor  $FT^{Icap}$  (eq. 22) :

$$FT^{Icap} = 1 - e^{-\frac{1}{f^S} \times \mu^{Icap} \times \chi_{om}} \quad (22)$$

which  $\mu^{Icap}$  is the vegetable interception coefficient depending of the plant daily irrigation rate, and  $\chi_{om}$  is the dry biomass.

### 3.7. Limits of analysis

The choice of uncertain parameters implies a restriction of the conclusion to a partial domain of the possible uncertainty. For instance, the current version of the TOCATTA model used the Rothamsted model to simulate the evolution of the organic carbon in the soil (Jenkinson, 1990; Jenkinson *et al.*, 1992). This model considers biodegradation kinetics by soil microbial activity for different organic carbon pools. The biodegradation parameters have been determined through a large number of long-term experimental tests. The parameters, however, can propagate a very large uncertainties in residence time of carbon in soils. In this scenario we have not considered as uncertain these sub-model parameters. Therefore

the results obtained in the present study do not encompass all the potential sources of the uncertainty of the TOCATTa model.

The USDA triangle describing the soil texture following a classification determined by the percentage of sand, silt and clay fractions is based on a granulometry considering that clay contains particles with diameters lower than 0.002 mm silt between 0.002 and 0.05 mm and sand between 0.05 and 2 mm. However other classification could be preconised notably by the IAEA based on the same granulometry but with an other terminology. The USDA soil taxonomy and WRB (World Reference Base for Soil Resources) soil classification systems use 12 textural classes whereas the UK-ADAS (UK-based independent agricultural and environmental consultancy) system uses 11 (Soil Science Division Staff, 2011). We think that the impact of the choice of french classification (Tabor, 2001) or UK-ADAS, WRB or USDA classification is less important with regards to the other uncertainties taken into account.

Whereas the Sobol' method was time consuming, the application of response surfaces with neural networks was efficient. Actually the efficient factor (EF) and the geometrical ratio index (GRI) for the different response surfaces were close to 1 for all variables (Table 4) except perhaps for the ingestion dose due to  $^{110m}\text{Ag}$  for which the efficient factors were rather around 0.85. However, our results of Sobol' method were based on the 12 most influential parameters obtained with Morris method with the total ingestion dose in  $^{14}\text{C}$ , in  $^{110m}\text{Ag}$  and in  $^3\text{H}$  plus 4 other input parameters in order to check a non-influential parameter. Therefore, we cannot compare strictly the results of Sobol' method and Morris or Spearman method for the total groundshine dose due to  $^{14}\text{C}$  because the parameter soil dry bulk density ( $X_{18}$ ) which is influential with Morris or Spearman method is not present in the input parameters of the Sobol' method.

#### 4. Summary and conclusions

This paper addressed the methodology of sensitivity analysis in a radiological dose assessment of the discharges of a nuclear power plant. This work puts in light the differences between the Spearman, Morris and Sobol' sensitivity methods.

For the total annual dose for all pathways, the nine most influential variables are the same for all three methods, but the rankings are very similar between Sobol' and Spearman and very different between Sobol' and Morris:

Between Sobol' and Spearman the first three variables are the same, as well as the fifth and ninth. Ranking inversion occur for ranks 4, 6, 7 and 8. Between Sobol' and Morris, no variable is ranked the same way, and variables that are very influential for Sobol' (notably the volatilisation rate constant ( $X_{44}$ ), the soil layer solid liquid distribution in  $^{14}\text{C}$  ( $X_{43}$ )) become much less influential for Morris and vice versa.

For the total ingestion dose due to  $^{14}\text{C}$ , the three methods (Spearman, Morris and Sobol') provide the same influential parameters ranked from the most to the least influential parameter: the dissolved inorganic carbon concentration ( $X_{14}$ ), the volatilisation rate constant ( $X_{44}$ ), the soil layer solid liquid distribution in  $^{14}\text{C}$  ( $X_{43}$ ) the dry matter fraction in fruit vegetable ( $X_{11}$ ), the respiratory recycling index in fruit vegetable ( $X_{38}$ ), the fish water content ( $X_6$ ), the plant daily irrigation rate in fruit vegetable ( $X_3$ ), the water infiltration ( $X_{16}$ ). The lack of consideration of the distribution law form of input parameters by the Morris method could explain the different ranking of these parameters between Sobol' and Morris methods. As a consequence, the Spearman method appears to be the most reliable and practical method with regards to the capability of ranking influential parameters for total ingestion dose and ingestion and groundshine dose due to  $^{14}\text{C}$  as well, and its easiness of its application in SYMBIOSE platform. In fact, in SYMBIOSE, stock and flow equations are generally first-order differential equations with simple parameterization with no non-linearity, but some model as in the soil system in interaction with plant system, is not totally monotonic. If the models were non monotonic the Spearman method would not be

the reliable method.

Sobol's method is the reference to keep and can be easily implemented on a meta-model generated for example by a neural network. The use of Spearman's method remains efficient in cases of little non-monotonicity. However, in cases where a strong non-monotonicity of the models is identified, it is advisable to carry out a sensitivity analysis with the Morris method to quickly identify the most influential variables and then carry out a Sobol' analysis on these variables to know their exact ranking.

## Acknowledgments

These studies were funded by IRSN and Électricité de France within the collaboration program GGP-environment, fiche action V1.101.2. This work was used and revised within the frame of Working group 5 of the MODARIA international project from the IAEA.

- G. Baroni, S. Tarantola. A general probabilistic framework for uncertainty and global sensitivity analysis of deterministic models: a hydrological case study *Environ. Model. Softw.*, 51 (2014), pp. 26-34, 10.1016/j.envsoft.2013.09.022 <http://www.sciencedirect.com/science/article/pii/S1364815213002211>
- Belot, Y., Roy, M., Métivier, H., 1996. *Le TRITIUM de l'Environnement à l'Homme* Collection IPSN, Les Edition de Physique, France.
- Bergmeir, C. & Benetez, J. (2012). Neural networks in R using the stuttgart neural network simulator: Rsnns. *Journal of Statistical Software*, 46(1):1–26.
- Borgonovo, E., & Plischke, E. (2016). Sensitivity analysis: a review of recent advances. *European Journal of Operational Research*, 248(3), 869-887.
- Bratley, P., Fox, B.L. (1988). Algorithm 659: Implementing Sobol's Quasirandom Sequence Generator. *ACM Transactions on Mathematical Software.*, 14:88–100.
- Breshears, David D., & Kirchner, Thomas B. & Whicker, F. Ward (1992). Contaminant transport through agroecosystems: assessing relative importance of environmental, physiological, and management factors. *Ecological Applications.*, 2(3):285–297.
- Campolongo, F., Cariboni, J. & Saltelli, A. (2007). An effective screening design for sensitivity. *Environmental Modelling & Software.*, 22:1509–1518.
- Choi, S. C. (1977). Tests of Equality of Dependent Correlation Coefficients *Biometrika*, 4 (3): 645–647. doi:10.1093/biomet/64.3.645.
- Ciffroy, P., Siclet, F., Damois, C., Muck, M., 2006. A dynamic model for assessing radiological consequences of tritium routinely released in rivers. Application to the Loire River. *J. Environ. Radioact.* 90, 110-139.

- Cosenza, A., Mannina, G., Vanrolleghem, P. A. & Neumann, M. B. (2013). Global sensitivity analysis in wastewater applications: A comprehensive comparison of different methods. *Environmental Modelling & Software*, 49:40 – 52.
- Davis, P. A., Kotzer, T. G., Workman, W. J. G. (2002). Environmental Tritium Concentrations due to continuous atmospheric sources. *Fus. Sci. Technol.*, 41:453–457.
- E. de Rocquigny, N. Devictor, and S. Tarantola, editors. *Uncertainty in industrial practice. A guide to quantitative uncertainty management*. Wiley, 2008.
- Fieller, E. C., Hartley, H. O., Pearson, E. S. (1957). Tests for rank correlation coefficients. I *Biometrika*, 44: 470–481. doi:10.1093/biomet/44.3-4.470
- D. Galeriu, A. Melintescu, N.A. Beresford, N.M.J. Crout, R. Peterson, H. Takeda, Modelling  $^3\text{H}$  and  $^{14}\text{C}$  transfer to farm animals and their products under steady state conditions, (2007) *Journal of Environmental Radioactivity*, Volume 98, Issues 1–2, 2007, Pages 205-217, ISSN 0265-931X, <https://doi.org/10.1016/j.jenvrad.2006.11.010>. (<http://www.sciencedirect.com/science/article/pii/S0265931X07001798>)
- Yanjun Gan, Qingyun Duan, Wei Gong, Charles Tong, Yunwei Sun, Wei Chu, Aizhong Ye, Chiyuan Miao, Zhenhua Di, A comprehensive evaluation of various sensitivity analysis methods: A case study with a hydrological model, *Environmental Modelling & Software*, Volume 51, 2014, Pages 269-285, ISSN 1364-8152, <https://doi.org/10.1016/j.envsoft.2013.09.031>. (<http://www.sciencedirect.com/science/article/pii/S1364815213002338>)
- Gibbons, J.D. & Chakraborti. S. (1992). *Nonparametric Statistical Inference* 3rd Ed. Marcel Dekker, New York
- Girard, S., Mallet, V., Korsakissok, I. & Mathieu, A. (2016). Emulation and Sobol' sensitivity analysis of an atmospheric dispersion model applied to the Fukushima nuclear accident *J. Geophys. Res. Atmos.*, 121, 3484–3496
- Greaver, T., Lobo Sternberg, L. d.S., Schaffer, B. and Moreno, T. (2005). An empirical method of measuring  $\{\text{CO}_2\}$  recycling by isotopic enrichment of respired  $\{\text{CO}_2\}$ . *Agricultural and Forest Meteorology*, 128(1-2):67 – 79.
- Hamby, D. M. (1994). A review of techniques for parameter sensitivity analysis of environmental models. *J. Environ. Monito. Assess.*, 32:135–154.
- Harris, C. M., Hoffman, K. L. & Yarrow, L.-A. (1995). Obtaining minimum-correlation Latin Hypercube Sampling plans using an IP-based heuristic. *OR Spektrum*, 17 :139–148.
- Herman, J. & Kollat, J. & Reed, P. & Wagener, Thorsten. (2013). Technical Note: Method of Morris effectively reduces the computational demands of global sensitivity analysis for distributed watershed models. *Hydrology and Earth System Sciences*. 17. 10.5194/hess-17-2893-2013.

- Hinton, T.G., Garnier-Laplace, J., Vandenhove, H., Dowdall, M., Adam-Guillermin, C., Alonzo, F., Barnett, C., Beaugelin-Seiller, K., Beresford, N.A., Bradshaw, C., Brown, J., Eyrolle, F., Fevrier, L., Gariel, J.C., Gilbin, R., Hertel-Aas, T., Horemans, N., Howard, B.J., Ikeheimonen, T., Mora, J.C., Oughton, D., Real, A., Salbu, B., Simon-Cornu, M., Steiner, M., Sweeck, L., Vives I Batlle, J., 2013. An invitation to contribute to a strategic research agenda in radioecology. *J. Environ. Radioact.*, 115:73–82.
- ICRP, 2006, Assessing Dose of the Representative Person for the Purpose of Radiation Protection of the Public and The Optimisation of Radiological Protection: Broadening the Process, ICRP Publication 101, Annals of the ICRP 36 (3), 2006.
- International Atomic Energy Agency, (2009) Quantification of Radionuclide Transfer in Terrestrial and Freshwater Environments for Radiological Assessments International Atomic Energy Agency, 2009
- International Atomic Energy Agency, (2010) Handbook of Parameter Values for the Prediction of Radionuclide Transfer in Terrestrial and Freshwater Environments International Atomic Energy Agency, 2010
- International Atomic Energy Agency, (2014) Guidelines for Using Fallout Radionuclides to Assess Erosion and Effectiveness of Soil Conservation Strategies International Atomic Energy Agency, 2014
- International Atomic Energy Agency (2014). Transfer of Tritium in the Environment after Accidental Releases from Nuclear Facilities. Report of Working Group 7. Tritium Accidents of Emras II Topical Heading. Approaches for Assessing Emergency Situations. Environmental Modelling for Radiation Safety (Emras II) Programme, TEC-DOC1738, IAEA, Vienne.
- Bertrand Iooss, Paul Lemaître. A review on global sensitivity analysis methods. C. Meloni and G. Dellino. Uncertainty management in Simulation-Optimization of Complex Systems: Algorithms and Applications, Springer, 2015. hal-00975701
- Jachner, S., van den Boogaart, K. G. & Petzoldt, T. (2007). Statistical methods for the qualitative assessment of dynamic models with time delay (r package qualv). *J. Stat. Soft.*, 22:1–30.
- Jean-Baptiste, P.; Fourré, E.; Baumier, D. & Dapoigny, A. (2011) Environmental OBT/TFWT Ratios Revisited Fusion Science and Technology, Taylor & Francis, 2011, 60, 1248-1251
- Jenkinson D. S., 1990. The turnover of organic carbon and nitrogen in soil. *Philos. Trans. R. Soc. B.*, 329: 361-368.
- Jenkinson D. S., D. D. Harkness, E. D. Vance, D. E. Adams and A. F. Harrison, 1992. Calculating net primary production and annual input of organic matter to soil from the amount and radiocarbon content of soil organic matter. *Soil Biol. Biochem.*, 24: 295-308.
- Kim, M. A. & Baumgartner, F. (1994). Equilibrium and non-equilibrium partition of tritium between organics and tissue water of different biological systems. *Appl. Radiat. Iso.*, 45:353–60.
- Le Dizes, S., Maro, D., Hebert, D., Gonze, M. A., Aulagnier, C. (2012). TOCATTA: a dynamic transfer

- model of  $^{14}\text{C}$  from the atmosphere to soil-plant systems. *J. Environ. Radioact.*, 105:48–59.
- Le Goff, P., Fromm, M., Vichot, L., Badot, P. M., Guetat, P. (2014). Isotopic fractionation of tritium in biological systems. *Environ. Int.*, (65):116–26.
- Limer, L. M. C. & Smith, K. & Albrecht, A. & Marang, L. & Norris, S. & Smith, G. M. & Thorne, M. C. & Xu, S. (2012). C-14 Long-Term Dose Assessment: Data Review, Scenario Development, and Model Comparison. Available at [www.stralsakerhetsmyndigheten.se](http://www.stralsakerhetsmyndigheten.se), 2012:47 ISSN:2000-0456
- McRae, G.J., Tilden, J.W., Seinfeld, J.H. (1982). Global sensitivity analysis—a computational implementation of the Fourier amplitude sensitivity test (FAST) *J. Comput. Chem. Eng.*, (6):15–25.
- Meyer, P. D. & Rockhold, M.L. & Nichols, W.E. & Gee, G.W. (1997). Hydrologic Evaluation Methodology for Estimating Water Movement Through the Unsaturated Zone at commercial Low-Level Radioactive Waste Disposal Sites NUREG/CR-6346 US-NRC Technical report.
- Meyer, P. D. & Rockhold, M.L. & Gee, G.W. (1997). Uncertainty Analyses of Infiltration and Subsurface Flow and Transport of SDMP Sites. NUREG/CR-6565 PNNL-11705 US-NRC Technical report.
- Meyer, P. D. & Orr, S. (2002). Evaluation of Hydrologic Uncertainty Assessments for Decommissioning Sites Using Complex and Simplified Models. NUREG/CR-6767 PNNL-13832 US-NRC Technical report.
- Mora, J.& Tellería, D.& Neaimi, A.& Buhr, A.& Bonchuk, Y.& Chouhan, S.& Chylý, P.& Curti, A.& Lauria, D.& Duran, J.& Galeriu, D.& Hägg, A.-C.& Heling, R.& Ivanis, G.& Iosjpe, M.& Krajewski, P.& Lager, C.& Marang, L.& Mourlon, C. & Zorko, B.(2014). MODARIA WG5: Towards a practical guidance for including uncertainties in the results of dose assessment of routine releases Conference: 3rd International Conference On Radioecology And Environmental Radioactivity (ICRER)
- Morris, M. D. (1991). Factorial sampling plans for preliminary computational experiments. *Technometrics*, 33:161–174.
- Nash, J. E. & Sutcliffe, V. (1970). River flow forecasting through conceptual models. Part I. A discussion of principles. *J. Hydrol.*, 10:282–290.
- Nicoulaud-Gouin, V., Garcia-Sanchez, L., Metivier, J.M., Gonze, M.A., 2014. Sensitivity analysis of a radionuclide transfer model describing contaminated vegetation in Fukushima prefecture, using Morris and Sobol’ indices. 3rd International Conference on Radioecology & Environmental Radioactivity (ICRER). 7-12 September 2014, Barcelona, Spain.
- V. Nicoulaud-Gouin, L. Garcia-Sanchez, M. Giacalone, J.C. Attard, A. Martin-Garin, F.Y. Bois, Identifiability of sorption parameters in stirred flow-through reactor experiments and their identification with a Bayesian approach, *Journal of Environmental Radioactivity*, Volumes 162–163, 2016, Pages 328-339, ISSN 0265-931X, <https://doi.org/10.1016/j.jenvrad.2016.06.008>.
- Pianosi, F., Beven, K., Freer, J., Hall, J. W., Rougier, J., Stephenson, D. B., & Wagener, T. (2016). Sensitivity analysis of environmental models: A systematic review with practical workflow. *Environmental*

- Modelling & Software, 79, 214-232.
- Pujol, G. (2016). sensitivity: Sensitivity Analysis. R package version 1.12-2.
- R Development Core Team (2012). R: a language and environment for statistical computing. R Foundation for Statistical Computing, Vienna, Austria. ISBN 3-900051-07-0.
- H. Renard, D. Maro, S. Le Dizès, A. Escobar-Gutiérrez, C. Voiseux, L. Solier, D. Hébert, M. Rozet, C. Cossonnet, R. Barillot (2017) Tritium forms discrimination in ryegrass under constant tritium exposure: From seed germination to seedling autotrophy, Journal of Environmental Radioactivity, Volume 177, Pages 194-205, ISSN 0265-931X, <https://doi.org/10.1016/j.jenvrad.2017.06.026>. (<http://www.sciencedirect.com/science/article/pii/S0265931X17303909>)
- Lisa Rivalin, Pascal Stabat, Dominique Marchio, Marcello Caciolo, Frédéric Hopquin, A comparison of methods for uncertainty and sensitivity analysis applied to the energy performance of new commercial buildings, Energy and Buildings, Volume 166, 2018, Pages 489-504, ISSN 0378-7788, <https://doi.org/10.1016/j.enbuild.2018.02.021>. (<http://www.sciencedirect.com/science/article/pii/S0378778818305243>)
- Ruano, M., Ribes, J., Seco, A. & Ferrer, J. (2012). An improved sampling strategy based on trajectory design for application of the morris method to systems with many input factors. Environmental Modelling & Software, 37:103 – 109.
- Saltelli, A., Chan, K. & Scott, M., éditeurs (2000). Sensitivity analysis. John Wiley and Sons, New York.
- Saltelli, A. (2002). Making best use of model evaluations to compute sensitivity indices. Computer Physics Communications, 145:280–297.
- Saltelli, A., 2017. Sensitivity analysis. PhD-course Numbers for policy: Practical problems in quantification Bergen, March 13–17, 2017. [http : //www.andreasaltelli.eu/file/repository/Bergen\\_Andrea\\_T\\_hursdays\\_A.pdf](http://www.andreasaltelli.eu/file/repository/Bergen_Andrea_T_hursdays_A.pdf).
- Sheppard SC, Sheppard MI, Siclet F. (2006) Parameterization of a dynamic specific activity model of <sup>14</sup>C transfer from surface water-to-humans. J Environ Radioact. 2006;87(1):15-31. doi: 10.1016/j.jenvrad.2005.10.006. Epub 2005 Dec 27. PMID: 16377038.
- Simon-Cornu, M., Beaugelin-Seiler, K., Boyer, P., Calmon, P., Garcia-Sanchez, L., Mourlon, C., Nicoulaud-Gouin, V., Gonze, M. A., Sy, M. M. (2015). Evaluating variability and uncertainty in radiological impact assessment using SYMBIOSE. J. Environ. Radioact., 139: 91–102 .
- Sin, G., Gernaey, K. V., Neumann, M. B., van Loosdrecht, M. C. & Gujer, W. (2011). Global sensitivity analysis in wastewater treatment plant model applications: Prioritizing sources of uncertainty. Water Research, 45(2):639 – 651.
- Soil Science Division Staff. 2017. Soil survey sand. C. Ditzler, K. Scheffe, and H.C. Monger (eds.). USDA Handbook 18. Government Printing Office, Washington, D.C.

- Xiao-meng Song, Fan-zhe Kong, Che-sheng Zhan, Ji-wei Han, Xin-hua Zhang, Parameter identification and global sensitivity analysis of Xin'anjiang model using meta-modeling approach, *Water Science and Engineering*, Volume 6, Issue 1, 2013, Pages 1-17, ISSN 1674-2370, <https://doi.org/10.3882/j.issn.1674-2370.2013.01.001>. (<http://www.sciencedirect.com/science/article/pii/S1674237015302210>)
- Spearman, C. (1904). The proof and measurement of correlation between two things *American Journal of Psychology*, 15 :72 – 101.
- Sy, Mouhamadou Moustapha, Gonze, M. A., Metivier, J. M., Nicoulaud-Gouin, V. & Simon-Cornu, M. (2016). Uncertainty analysis in post-accidental risk assessment models: An application to the Fukushima accident. *Annals of Nuclear Energy*, 93:94 – 106.
- Tabor, J. 2001. *Soil Classification Systems. Aridic Soils of the United States and Israel*. Tucson, AZ: Office of Arid Lands Studies, The University of Arizona.
- Laura Urso, Cagatay Ipbüker, Koit Muring, Hanno Ohvri, Martin Vilbaste, Marko Kaasik, Alan Tkaczyk, Justin Brown, Ali Hosseini, Mikhail Iosjpe, Ole Christian Lind, Brit Salbu, Philipp Hartmann, Martin Steiner, Juan Carlos Mora, Danyl Pérez-Sánchez, Almudena Real, Justin Smith, Christophe Mourlon, Pedram Masoudi, Marc-André Gonze, Mathieu Le Coz, Khaled Brimo, Jordi Vives i Batlle (2019) *TERRITORIES D9.62 Guidance on Uncertainty Analysis for Radioecological Models*. CONCERT deliverables
- USDA (2008). *Soil quality indicators- Bulk density*. USDA NRCS.
- Weil, R. R. & Brady, N. C. (2016). *The nature and properties of soils*. 15th edition Pearson.
- Xie, Y. (2011). *animation: A Gallery of Animations in Statistics and Utilities to Create Animations*. R package version 2.0-3. <https://github.com/brentertz/scianimator>
- Xue, C. & Gertner, G. (2011). Understanding and comparisons of different sampling approaches for the Fourier Amplitudes Sensitivity Test (FAST) *J. Comput. Stat. Data Anal.*, 55(1):184–198. doi:10.1016/j.csdq.2010.06.028.
- Zell, A. & Mamier, G. & Vogt, M. & Mache, N. & Hebner, R. & Dering, S. & Herrmann, K.-U. & Soyez, T. & Schmalzl, M. & Sommer, T. & Hatzigeorgiou, A. & Posselt, D. & Schreiner, T. & Kett, B. & Clemente, G. & Wieland, J.(1998). *SNNS Stuttgart Neural Network Simulator User Manual, Version 4.2*. IPVR, University of Stuttgart and WSI, University of Tebingen. <http://www.ra.cs.uni-tuebingen.de/SNNS/>

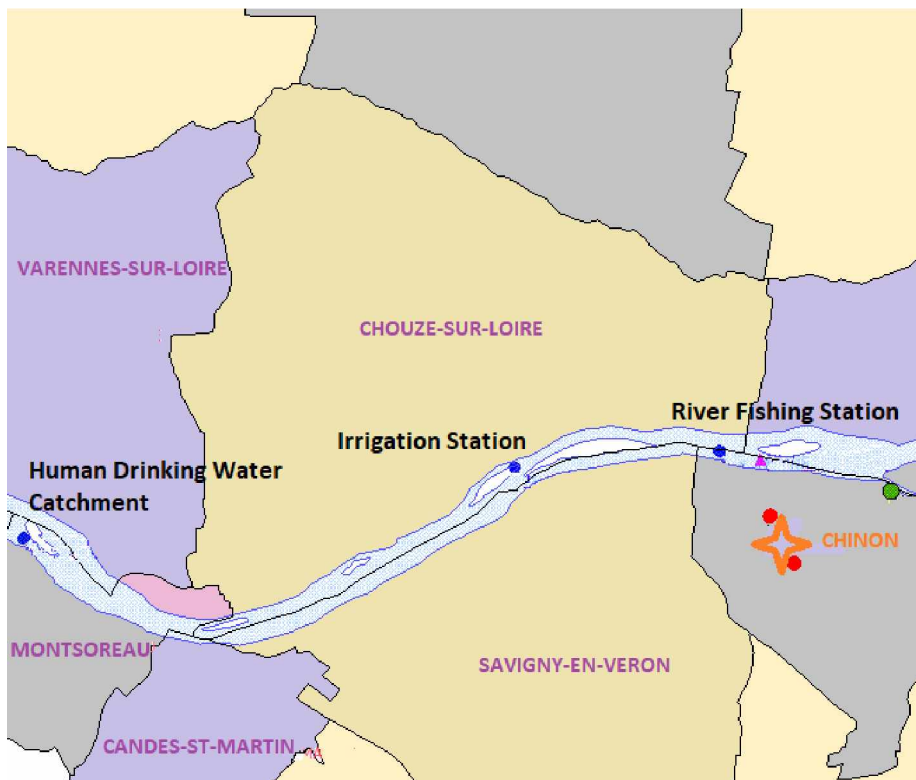


Figure 1: Landscape of Chinon nuclear power plant (with its 2 stacks, red dots) with the three river receptor points (blue dots) and the location (green dot) at which the sensitivity analysis has been operated (from GeoSymbiose)

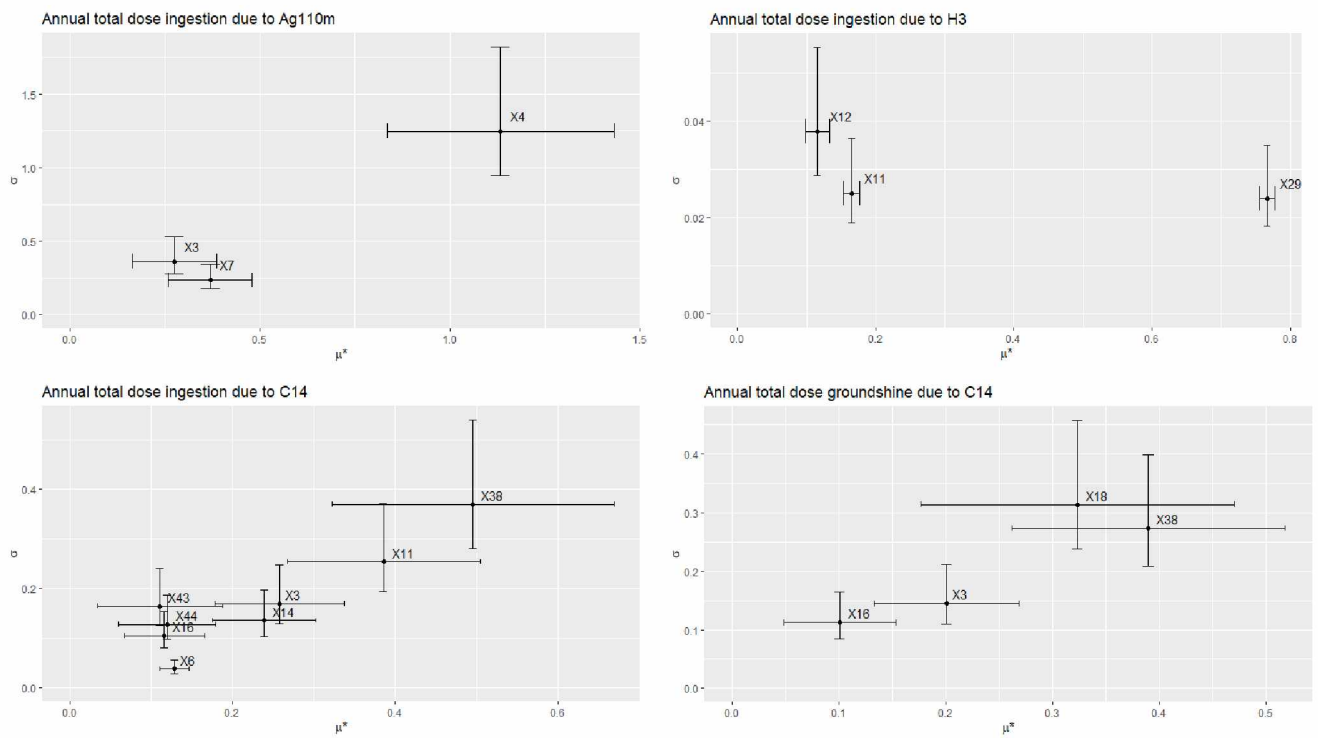


Figure 2: Morris plots for variable Annual total ingestion dose due to  $^{110m}\text{Ag}$  at the top left, for variable Annual total ingestion dose due to  $^3\text{H}$  at the top right, for variable Annual total ingestion dose due to  $^{14}\text{C}$  at the bottom left and for variable Annual total groundshine dose due to  $^{14}\text{C}$  at the bottom right

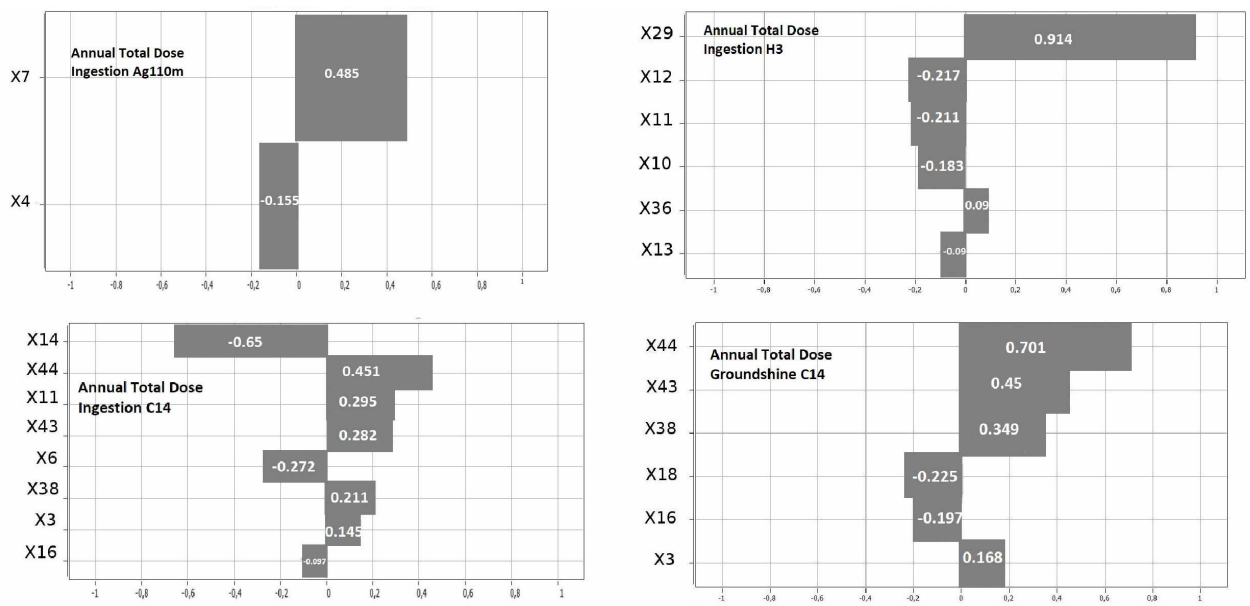


Figure 3: Spearman Tornado Charts for variable Annual total ingestion dose due to <sup>110m</sup>Ag at the top left, for variable Annual total ingestion dose due to <sup>3</sup>H at the top right, for variable Annual total ingestion dose due to <sup>14</sup>C at the bottom left and for variable Annual total groundshine dose due to <sup>14</sup>C at the bottom right

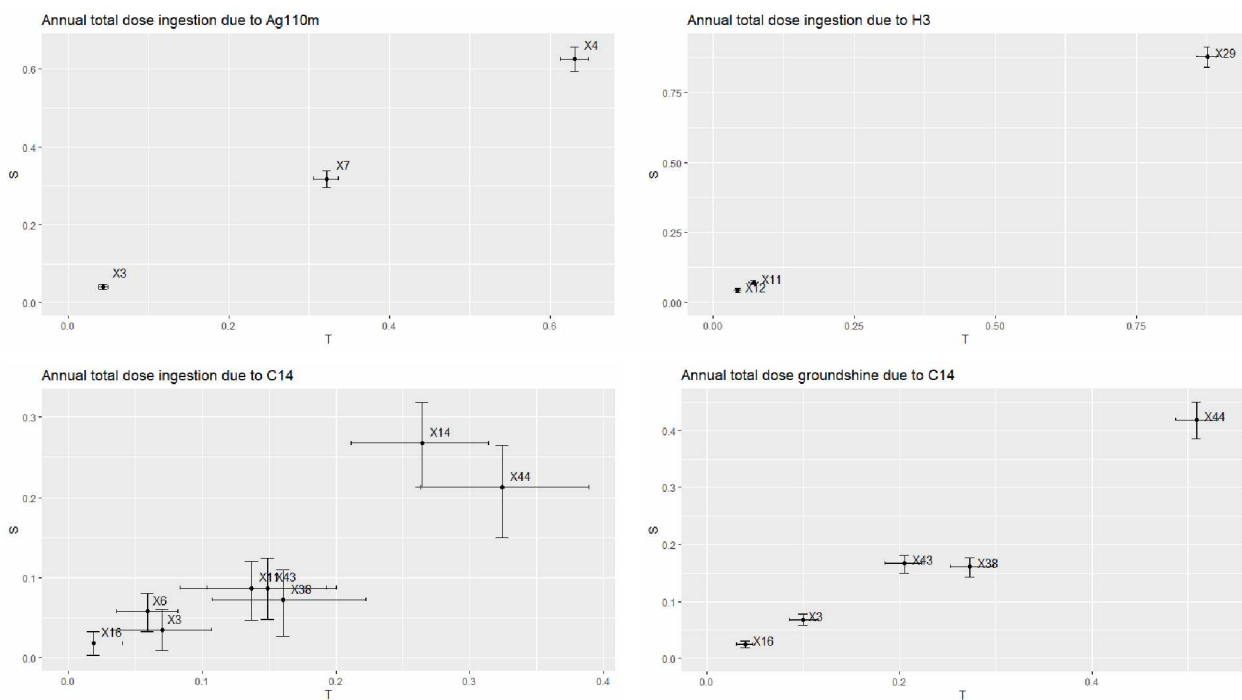


Figure 4: Sobol' plot (First indices  $S_i$  over Total indices  $T_i$ ) for variable Annual total ingestion dose due to  $^{110m}\text{Ag}$  at the top left, for variable Annual total ingestion dose due to  $^3\text{H}$  at the top right, for variable Annual total ingestion dose due to  $^{14}\text{C}$  at the bottom left and for variable Annual total groundshine dose due to  $^{14}\text{C}$  at the bottom right

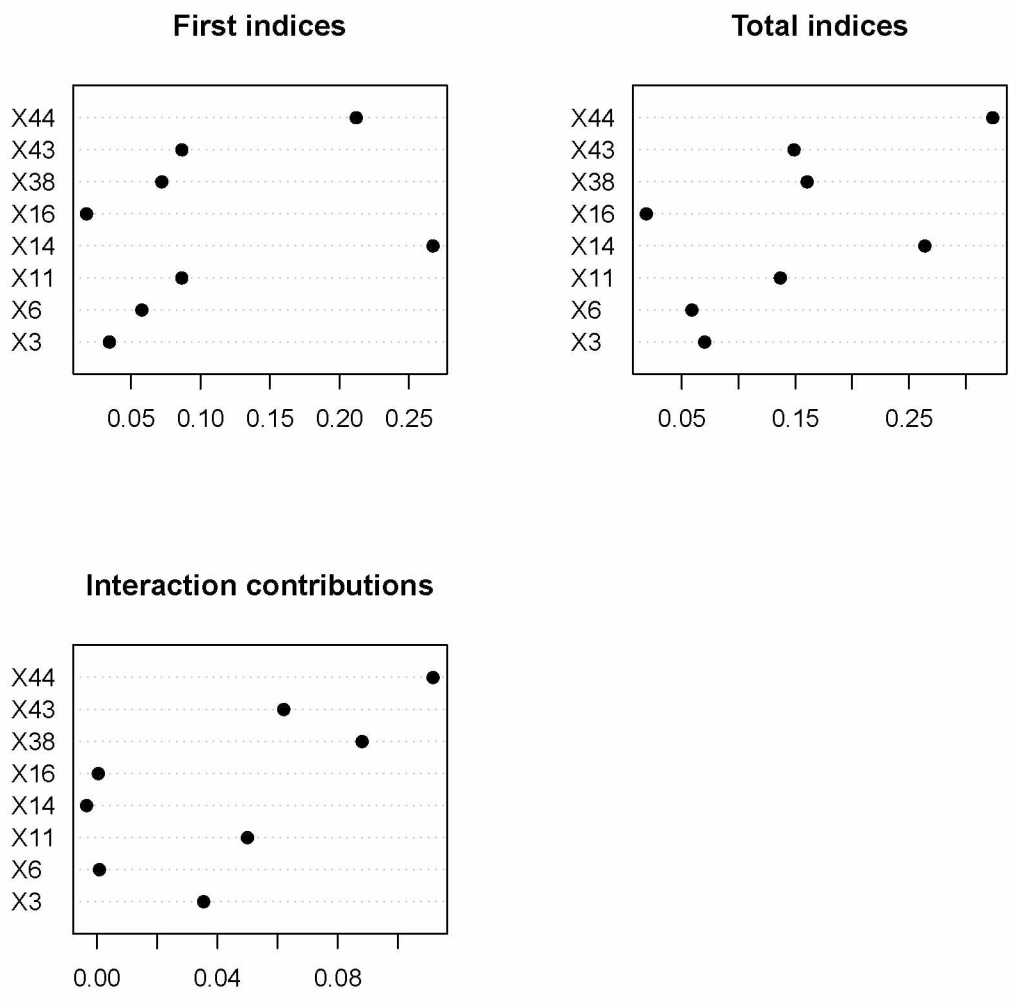


Figure 5: Sobol' results at the last time represented by dotcharts for ingestion dose in  $^{14}\text{C}$ . First indices at the top left, Total indices at the top right and the difference between Total indices and First indices representing the contribution of interactions at the bottom.

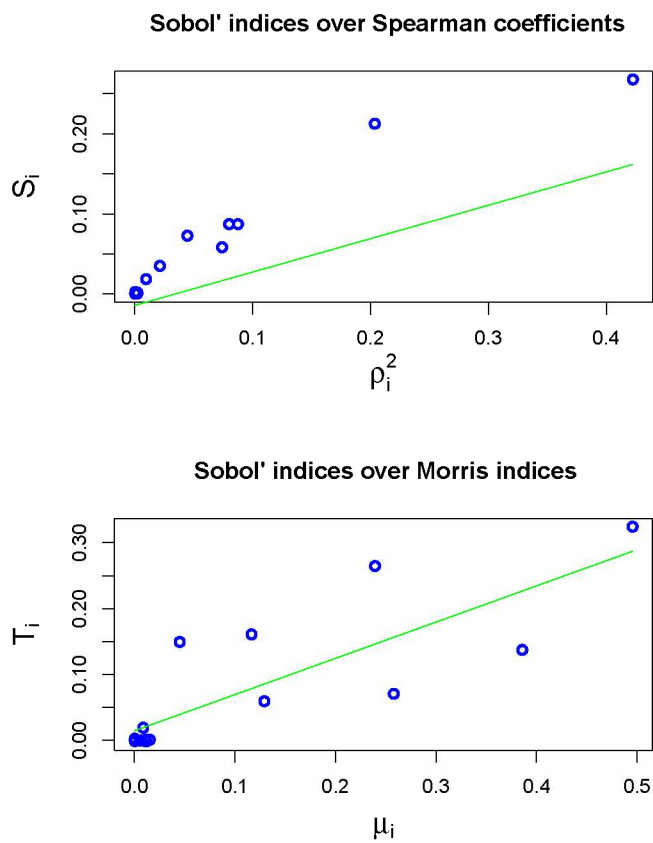


Figure 6: Scatter plots of sensitivity indices of the ingestion dose due to  $^{14}\text{C}$  at last time. Sobol' first indices over Spearman coefficients at the top, Sobol' total indices over Morris indices  $\mu^*$  at the bottom.

Table 1: Hierarchical interaction matrix between sub-systems of the biosphere in simulator Biosphere of the platform Symbiose

Discharge $^3\text{HTO}$ $^{14}\text{C}_{\text{min}}$ $^{14}\text{C}_{\text{org}}$ $^{110\text{m}}\text{Ag}$	Atmo dis-charge $^3\text{HTO}$ $^{14}\text{C}_{\text{min}}$ $^{14}\text{C}_{\text{org}}$	River discharge $^3\text{HTO}$ $^{14}\text{C}_{\text{min}}$ $^{110\text{m}}\text{Ag}$				
	Atmo system	Rain	Rain	Rain		External (plumeshine)
		River system	Irrigation / watering	Irrigation / watering	Pumping	External (groundshine)
			Agricultural System / $^{110\text{m}}\text{Ag}$		Collecting	External (groundshine)
				Agricultural System / TOCATTA ( $^{14}\text{C}$ , $^3\text{H}$ )	Collecting	Inhalation External (groundshine)
					Dietary System	Ingestion
						Man Dose (Rural adult)

Table 2: Deterministics data

Subsystem of the biosphere see cells on the diagonal of Table 1	Input data	Source or Reference
River system	Liquid discharges from the Chinon NPP under normal operating conditions for the year 2011. River flow rates: monthly averaged daily measurements at the Langeais station in 2011, approximately 20 km upstream the Chinon NPP River temperature and river suspended matter load: one value per month in 2011 at the Chouzé station, located in the first kilometers downstream the NPP. Bicarbonates load: 2011 values for 3 stations, close to Chinon NPP (Langeais, Chouzé and Avoine)	EDF (measurement or calculation)  DREAL Centre, HYDRO database (French Ministry of Ecology)  Osur Web, managed by the Loire-Bretagne water agency ( <a href="http://www.eau-loire-bretagne.fr/informations_et_donnees/donnees_brutes/osur_web">http://www.eau-loire-bretagne.fr/informations_et_donnees/donnees_brutes/osur_web</a> ). Osur web, op.cit.
Atmospheric system	Atmospheric discharges from the Chinon NPP under normal operating conditions for the year 2011. For both stacks: height, diameter, discharge temperature and release velocity Hourly values for year 2011 of: wind direction, wind speed, rainfall, atmospheric boundary layer height. Hourly values for year 2011 of cloud cover.	EDF (measurement or calculation)  EDF  EDF (meteorological station of Chinon NPP)
Agricultural system	Daily temperature averages station of Tours in 2011	EDF Meteo France meteorological station of Tours Meteo France <a href="https://donneespubliques.meteofrance.fr/?fond=produit&amp;id_produit=90&amp;id_rubrique=32">https://donneespubliques.meteofrance.fr/?fond=produit&amp;id_produit=90&amp;id_rubrique=32</a>
Dietary system and Man	Collecting of drinking water assumed to originate from water river 9km downstream the liquid discharge outlet. Collecting of irrigation water assumed to originate from river water 3 km downstream the NPP. In both cases, real catchments are in alluvial aquifer downstream, and the participants assumed that this was river water, neglecting river-aquifer exchanges. Local food consumption rate for adults with the highest local food consumption in the vicinity of the Chinon NPP Time use: data for region Centre of France	Collective choices of the MODARIA group based on observations and hypotheses  Parache, 2011  CIBLEX database (IRSN, 2003)

Table 3: Uncertain input parameters laws and variation domain.

Parameter	Name	Law	Min	Max	Truncature or mode	Reference
$X_1$	Annual crop daily irrigation rate (mm) in animal spring cereal	Uniform	0	2.4		(IAEA, 2009)
$X_2$	Annual crop daily irrigation rate (mm) in animal winter cereal	Uniform	0	2.4		(IAEA, 2009)
$X_3$	Plant daily irrigation rate (mm) in fruit vegetable	Uniform	2	6		(IAEA, 2009)
$X_4$	Plant daily irrigation rate (mm) in leafy vegetable	Uniform	2	6		(IAEA, 2009)
$X_5$	Plant daily irrigation rate (mm) in root vegetable	Uniform	2	6		(IAEA, 2009)
$X_6$	Fish water content ( $m^3.kg^{-1}$ )	Normal truncated	0.000728	0.000852	0.99	(Sheppard <i>et al.</i> , 2006)
$X_7$	Reference coefficient partition ( $m^3.kg^{-1}$ ) of Ag in suspended matter	Log normal truncated	16.1	450	0.95	(Simon-Cornu <i>et al.</i> , 2015)
$X_8$	Animal feedstuff annual crop dry matter fraction (-) in animal spring cereal	Uniform	0.84	0.9		(IAEA, 2010)
$X_9$	Animal feedstuff annual crop dry matter fraction (-) in animal winter cereal	Uniform	0.84	0.9		(IAEA, 2010)
$X_{10}$	Animal feedstuff annual crop dry matter fraction (-) in root and tuber	Uniform	0.18	0.38		(IAEA, 2010)
$X_{11}$	Vegetable dry matter fraction (-) in fruit vegetable	Uniform	0.03	0.16		(IAEA, 2010)
$X_{12}$	Vegetable dry matter fraction (-) in leafy vegetable	Uniform	0.03	0.16		(IAEA, 2010)
$X_{13}$	Vegetable dry matter fraction (-) in root vegetable	Uniform	0.05	0.23		(IAEA, 2010)
$X_{14}$	Water dissolved inorganic carbon concentration ( $kg.m^{-3}$ ) in human drinking water catchment	Log normal truncated	0.01231	0.03578	0.95	This study
$X_{15}$	Reference coefficient partition ( $m^3.kg^{-1}$ ) of Ag in sandy soil	Log uniform	0.036	15		pdf fitted on Loire river data (Simon-Cornu <i>et al.</i> , 2015)
$X_{16}$	Water infiltration rate ( $mm.h^{-1}$ ) in sandy soil	Normal truncated	0.424272	5.53186	0.999	(Meyer <i>et al.</i> , 1997)
$X_{17}$	Soil layer volumetric water content ( $m^3.m^{-3}$ ) in sandy soil	Normal truncated	0.132	0.688	0.999	(Meyer <i>et al.</i> , 1997)
$X_{18}$	Soil dry density <sup>2</sup> ( $kg.m^{-3}$ ) in sandy soil	Normal truncated	632.88	2000	0.999	(Meyer & Orr, 2002)
$X_{19}$	Organ stable carbon concentration ( $mol.kg^{-1}$ ) in chicken meat	Normal truncated	29.6	48.6	0.99	(Galeriu <i>et al.</i> , 2007)
$X_{20}$	Organ stable carbon concentration ( $mol.kg^{-1}$ ) in hen egg	Normal truncated	34.4	56.6	0.99	(Galeriu <i>et al.</i> , 2007)
$X_{21}$	Biological elimination rate of OBT ( $d^{-1}$ ) in chicken	Triangular	0.002	0.012	0.007	(Belot <i>et al.</i> , 1996)
$X_{22}$	Phytoplankton stable carbon concentration ( $kg.kg^{-1}$ )	Normal truncated	0.436	0.564	0.99	(Sheppard <i>et al.</i> , 2006)
$X_{23}$	Fish stable carbon concentration ( $kg.kg^{-1}$ )	Normal truncated	0.434	0.526	0.99	(Sheppard <i>et al.</i> , 2006)
$X_{24}$	Fish stable hydrogen concentration ( $kg.kg^{-1}$ )	Uniform	0.055	0.085		(Ciffroy <i>et al.</i> , 2006)
$X_{25}$	Phytoplankton isotopic discrimination factor (-) in $H^3$	Uniform	0.38	0.54		(IAEA, 2014)
$X_{26}$	Fish depuration rate ( $d^{-1}$ )	Uniform	5	10		(Ciffroy <i>et al.</i> , 2006)
$X_{27}$	Fish equilibrium concentration factor (-) in OBT	Log triangular	0.03	0.9	0.4	(Ciffroy <i>et al.</i> , 2006)
$X_{28}$	Fish threshold temperature (K)	Uniform	279	281		(Ciffroy <i>et al.</i> , 2006)
$X_{29}$	Vegetable isotopic discrimination (-) of $H^3$ in fruit vegetable	Log triangular	0.77	1.28	0.9	(Le Goff <i>et al.</i> , 2014)
$X_{30}$	Vegetable stable carbon concentration ( $mol.kg^{-1}$ ) in fruit vegetable	Normal truncated	29.8	38.6	0.99	(Galeriu <i>et al.</i> , 2007)
$X_{31}$	Vegetable stable carbon concentration ( $mol.kg^{-1}$ ) in leafy vegetable	Normal truncated	29.8	38.6	0.99	(Galeriu <i>et al.</i> , 2007)
$X_{32}$	Vegetable stable carbon concentration ( $mol.kg^{-1}$ ) in root vegetable	Normal truncated	29.8	38.6	0.99	(Galeriu <i>et al.</i> , 2007)
$X_{33}$	Annual crop isotopic discrimination (-) of $H^3$ in animal spring cereal	Log triangular	0.73	1.08	0.9	(Le Goff <i>et al.</i> , 2014)
$X_{34}$	Annual crop stable carbon concentration ( $mol.kg^{-1}$ ) in animal spring cereal	Normal truncated	32.4	44.2	0.99	(Galeriu <i>et al.</i> , 2007)
$X_{35}$	Annual crop stable carbon concentration ( $mol.kg^{-1}$ ) in animal winter cereal	Normal truncated	32.4	44.2	0.99	(Galeriu <i>et al.</i> , 2007)
$X_{36}$	Annual crop stable carbon concentration ( $mol.kg^{-1}$ ) in root and tuber	Normal truncated	29.8	38.6	0.99	(Galeriu <i>et al.</i> , 2007)
$X_{37}$	Annual crop respiratory recycling index (-) in animal spring cereal	Triangular	0.33	0.71	0.45	(Limer <i>et al.</i> , 2012)
$X_{38}$	Vegetable respiratory recycling index (-) in fruit vegetable	Triangular	0.03	0.29	0.12	(Limer <i>et al.</i> , 2012)
$X_{39}$	Soil to plant transfer factor (-) in sandy soil and fruit vegetable for Ag	Log uniform	0.00025	0.002		(Simon-Cornu <i>et al.</i> , 2015)
$X_{40}$	Soil to plant transfer factor (-) in sandy soil and leafy vegetable for Ag	Log uniform	5.9e-05	0.0013		(Simon-Cornu <i>et al.</i> , 2015)
$X_{41}$	Soil to plant transfer factor (-) in sandy soil and root vegetable for Ag	Log uniform	0.00057	0.0039		(Simon-Cornu <i>et al.</i> , 2015)
$X_{42}$	Soil layer clay plus silt fraction (-) in sandy soil	Triangular	0.15	0.5	0.17	This study
$X_{43}$	Soil layer solid liquid distribution coefficient ( $m^3.kg^{-1}$ ) in sandy soil in $^{14}C$	Log normal truncated	0.00053	0.0148	0.95	(Sheppard <i>et al.</i> , 2006)
$X_{44}$	Volatilisation rate constant ( $d^{-1}$ )	Log normal truncated	0.004	0.41	0.95	(Sheppard <i>et al.</i> , 2006)
$X_{45}$	Soil layer porosity ( $m^3.m^{-3}$ ) in sandy soil	Normal truncated	0.153	0.628	0.999	(Meyer <i>et al.</i> , 1997)
$X_{46}$	Annual crop soil layer surface exchange velocity HTO ( $m.s^{-1}$ ) in animal spring cereal	Log triangular	0.001	0.01	0.0012	(IAEA, 2014)
$X_{47}$	Vegetable soil layer surface exchange velocity HTO ( $m.s^{-1}$ ) in fruit vegetable	Log triangular	0.001	0.01	0.0012	(IAEA, 2014)

Table 4: goodness of fit of the response surfaces based on neural networks on the test sample for all the studied variables. GRI : geometric reliability index, EF : efficiency factor

Variable	Date	GRI	EF
Ingestion dose due to $^{110m}\text{Ag}$	Annual Dose 2011	1.007	0.832
Ingestion dose due to $^3\text{H}$	Annual Dose 2011	1.003	0.995
External groundshine dose due to $^{14}\text{C}$	Annual Dose 2011	1.001	0.927
Ingestion dose due to $^{14}\text{C}$	Annual Dose 2011	1.07	0.968

Table 5: Position factor on the 8 influential input parameters for annual ingestion dose in  $^{14}\text{C}$ . The maximum value of a position factor for 8 parameters is 7.11

Position Factor	annual ingestion dose in $^{14}\text{C}$ on 2011
$PF_{Morris-Sobol}$	5.65
$PF_{Spearman-Sobol}$	3.20

Table 6: Most influential parameters in the sensitivity analysis for the annual total dose for all pathways and all radionuclides : Morris indices  $\mu_i^*$  and Spearman indices  $\rho_i$ , first Sobol' indices  $S_i$ , and Total Sobol' indices  $T_i$ , sorted by Spearman indices.

Variable	Name	Morris $\mu^*$	Spearman $\rho$	Sobol S	Sobol T
$X_{14}$	Water dissolved inorganic carbon concentration ( $kg.m^{-3}$ )	0.237	-0.620	0.262	0.248
$X_{44}$	Volatilisation rate constant ( $d^{-1}$ )	0.119	0.445	0.225	0.313
$X_{43}$	Soil layer solid liquid distribution coefficient ( $m^3.kg^{-1}$ ) in sandy soil in $^{14}C$	0.110	0.277	0.085	0.139
$X_6$	Fish water content ( $m^3.kg^{-1}$ )	0.128	-0.266	0.060	0.049
$X_{11}$	Vegetable dry matter fraction (-) in fruit vegetable	0.361	0.243	0.072	0.105
$X_{29}$	Vegetable isotopic discrimination (-) of $H^3$ in fruit vegetable	0.104	0.220	0.039	0.023
$X_{38}$	Annual crop respiratory recycling index (-) in fruit vegetable	0.492	0.205	0.084	0.147
$X_3$	Plant daily irrigation rate (mm) in fruit vegetable	0.259	0.150	0.046	0.067
$X_{16}$	Water infiltration rate ( $mm.h^{-1}$ ) in sandy soil	0.123	-0.097	0.026	0.013
$X_{19}$	Organ stable carbon concentration ( $mol.kg^{-1}$ ) in chicken meat	0.003	-0.088	-	-
$X_{22}$	Phytoplankton stable carbon concentration ( $kg.kg^{-1}$ )	0.054	0.086	-	-
$X_9$	Animal feedstuff annual crop dry matter fraction (-) in animal winter cereal	$1.085 \cdot 10^{-4}$	0.083	-	-
$X_7$	Reference coefficient partition ( $m^3.kg^{-1}$ ) of Ag in suspended matter	0.036	0.065	0.011	0.0003
$X_{28}$	Fish threshold temperature (K)	$6.240 \cdot 10^{-6}$	0.058	-	-
$X_{35}$	Annual crop stable carbon concentration ( $mol.kg^{-1}$ ) in animal winter cereal	$4.206 \cdot 10^{-4}$	0.055	-	-
$X_{45}$	Soil layer porosity ( $m^3.m^{-3}$ ) in sandy soil	0.001	-0.048	-	-
$X_4$	Plant daily irrigation rate (mm) in leafy vegetable	0.010	-0.046	0.005	-0.003
$X_{17}$	Soil layer volumetric water content ( $m^3.m^{-3}$ ) in sandy soil	0.006	0.045	-	-
$X_{26}$	Fish depuration rate ( $d^{-1}$ )	$1.47 \cdot 10^{-6}$	-0.041	-	-
$X_{21}$	Biological elimination rate of OBT ( $d^{-1}$ ) in chicken	$2.21 \cdot 10^{-8}$	-0.035	-	-
$X_{37}$	Annual crop respiratory recycling index (-) in animal spring cereal	0.012	0.035	-	-
$X_{23}$	Fish stable carbon concentration ( $kg.kg^{-1}$ )	$3.590 \cdot 10^{-15}$	0.034	-	-
$X_{13}$	Vegetable dry matter fraction (-) in root vegetable	0.003	-0.033	0.003	-0.001
$X_{34}$	Annual crop stable carbon concentration ( $mol.kg^{-1}$ ) in animal spring cereal	0.001	-0.032	-	-
$X_{18}$	Soil dry density $^2$ ( $kg.m^{-3}$ ) in sandy soil	0.072	0.030	-	-
$X_2$	Annual crop daily irrigation rate (mm) in animal winter cereal	0.007	-0.025	-	-
$X_8$	Animal feedstuff annual crop dry matter fraction (-) in animal spring cereal	$1.274 \cdot 10^{-4}$	-0.025	-	-
$X_{25}$	Phytoplankton isotopic discrimination factor (-) in $H^3$	0.000	0.024	-	-
$X_{33}$	Annual crop isotopic discrimination (-) of $H^3$ in animal spring cereal	0.012	-0.023	-	-
$X_{41}$	Soil to plant transfer factor (-) in sandy soil and root vegetable for Ag	$2.03 \cdot 10^{-10}$	-0.023	-	-
$X_{36}$	Annual crop stable carbon concentration ( $mol.kg^{-1}$ ) in root and tuber	0.002	0.021	-	-
$X_{20}$	Organ stable carbon concentration ( $mol.kg^{-1}$ ) in hen egg	0.003	0.020	-	-
$X_{30}$	Vegetable stable carbon concentration ( $mol.kg^{-1}$ ) in fruit vegetable	0.005	-0.018	-	-
$X_5$	Plant daily irrigation rate (mm) in root vegetable	0.005	0.016	0.006	-0.005
$X_{40}$	Soil to plant transfer factor (-) in sandy soil and leafy vegetable for Ag	$2.85 \cdot 10^{-11}$	-0.015	-	-
$X_{39}$	Soil to plant transfer factor (-) in sandy soil and fruit vegetable for Ag	$1.39 \cdot 10^{-10}$	-0.013	-	-
$X_{27}$	Fish equilibrium concentration factor (-) in OBT	$3.995 \cdot 10^{-4}$	-0.009	-	-
$X_{32}$	Vegetable stable carbon concentration ( $mol.kg^{-1}$ ) in root vegetable	$4.923 \cdot 10^{-4}$	0.008	-	-
$X_{12}$	Vegetable dry matter fraction (-) in leafy vegetable	0.007	-0.008	0.008	-0.005
$X_{47}$	Vegetable soil layer surface exchange velocity HTO ( $m.s^{-1}$ ) in fruit vegetable	0.001	0.007	-	-
$X_{24}$	Fish stable hydrogen concentration ( $kg.kg^{-1}$ )	$7.8 \cdot 10^{-8}$	0.007	-	-
$X_{10}$	Animal feedstuff annual crop dry matter fraction (-) in root and tuber	0.002	-0.006	-	-
$X_{31}$	Vegetable stable carbon concentration ( $mol.kg^{-1}$ ) in leafy vegetable	0.001	0.006	-	-
$X_{46}$	Annual crop soil layer surface exchange velocity HTO ( $m.s^{-1}$ ) in animal spring cereal	$2.2 \cdot 10^{-8}$	0.005	-	-
$X_{15}$	Reference coefficient partition ( $m^3.kg^{-1}$ ) of Ag in sandy soil	$1.042 \cdot 10^{-4}$	0.004	0.010	-0.011
$X_{42}$	Soil layer clay plus silt fraction (-) in sandy soil	0.044	0.004	0.005	-0.003
$X_1$	Annual crop daily irrigation rate (mm) in animal spring cereal	0.015	0.002	-	-

Table 7: Most influential parameters in the sensitivity analysis for the ingestion dose in  $^{14}\text{C}$  variable: Morris indices  $\mu^*$  and Spearman indices  $\rho$  with confidence intervals.

parameters	median	[ 2.5 %, 97.5 %]
Morris indices $\mu^*$		
$X_{38}$	0.49	[0.32;0.66]
$X_{11}$	0.38	[0.26;0.50]
$X_3$	0.25	[0.17;0.33]
$X_{14}$	0.23	[0.17;0.30]
$X_6$	0.12	[0.11;0.14]
$X_{44}$	0.12	[0.06;0.17]
$X_{43}$	0.11	[0.03;0.18]
$X_{16}$	0.11	[0.06;0.16]
$X_{22}$	0.05	[0.04;0.06]
Spearman indices $\rho$		
$X_{14}$	-0.64	[-0.68;-0.61]
$X_{44}$	0.45	[0.39;0.49]
$X_{11}$	0.29	[0.23;0.35]
$X_{43}$	0.28	[0.22;0.33]
$X_6$	-0.27	[-0.32;-0.21]
$X_{38}$	0.21	[0.14;0.27]
$X_3$	0.14	[0.08;0.20]
$X_{16}$	-0.09	[-0.15;-0.03]
$X_{22}$	0.08	[0.02,0.14]

Table 8: Sobol' results for the ingestion dose in  $^{14}\text{C}$  variable: first and total indices with confidence intervals at the last simulation time. Negative values were due to numerical errors and were not relevant of influential parameters.

Parameters	name	First Index	min	max
$X_{14}$	Water dissolved inorganic carbon concentration	$2.68 \cdot 10^{-1}$	$2.13 \cdot 10^{-1}$	$3.19 \cdot 10^{-1}$
$X_{44}$	Volatilisation rate constant	$2.12 \cdot 10^{-1}$	$1.50 \cdot 10^{-1}$	$2.65 \cdot 10^{-1}$
$X_{11}$	Vegetable dry matter fraction in fruit vegetable	$8.69 \cdot 10^{-2}$	$4.74 \cdot 10^{-2}$	$1.21 \cdot 10^{-1}$
$X_{43}$	Soil layer solid liquid distribution coefficient for $^{14}\text{C}$	$8.69 \cdot 10^{-2}$	$4.85 \cdot 10^{-2}$	$1.24 \cdot 10^{-1}$
$X_{38}$	Vegetable respiratory recycling index in fruit vegetable	$7.24 \cdot 10^{-2}$	$2.63 \cdot 10^{-2}$	$1.10 \cdot 10^{-1}$
$X_6$	Fish water content	$5.81 \cdot 10^{-2}$	$3.31 \cdot 10^{-2}$	$8.06 \cdot 10^{-2}$
$X_3$	Plant daily irrigation rate in fruit vegetable	$3.48 \cdot 10^{-2}$	$9.56 \cdot 10^{-3}$	$5.98 \cdot 10^{-2}$
$X_{16}$	Water infiltration rate	$1.84 \cdot 10^{-2}$	$3.40 \cdot 10^{-3}$	$3.29 \cdot 10^{-2}$
$X_{29}$	Vegetable isotopic discrimination for H.3 in fruit vegetable	$2.20 \cdot 10^{-3}$	$1.12 \cdot 10^{-4}$	$4.19 \cdot 10^{-3}$
$X_{12}$	Vegetable dry matter fraction in leafy vegetable	$1.65 \cdot 10^{-3}$	$-2.72 \cdot 10^{-4}$	$3.58 \cdot 10^{-3}$
$X_{15}$	Distribution coefficient for sandy soil and Ag	$1.34 \cdot 10^{-3}$	$-5.87 \cdot 10^{-4}$	$3.33 \cdot 10^{-3}$
$X_5$	Plant daily irrigation rate in root vegetable	$1.20 \cdot 10^{-3}$	$-5.59 \cdot 10^{-4}$	$2.76 \cdot 10^{-3}$
$X_7$	Reference coefficient partition in matter	$1.16 \cdot 10^{-3}$	$-5.67 \cdot 10^{-4}$	$2.70 \cdot 10^{-3}$
$X_{42}$	Soil layer clay plus silt fraction	$5.29 \cdot 10^{-4}$	$-2.74 \cdot 10^{-3}$	$3.43 \cdot 10^{-3}$
$X_4$	Plant daily irrigation rate in leafy vegetable	$4.44 \cdot 10^{-4}$	$-1.67 \cdot 10^{-3}$	$2.44 \cdot 10^{-3}$
$X_{13}$	Vegetable dry matter fraction in root vegetable	$1.85 \cdot 10^{-4}$	$-1.91 \cdot 10^{-3}$	$2.12 \cdot 10^{-3}$
Parameters	name	Total Index	min	max
$X_{44}$	Volatilisation rate constant	$3.24 \cdot 10^{-1}$	$2.63 \cdot 10^{-1}$	$3.89 \cdot 10^{-1}$
$X_{14}$	Water dissolved inorganic carbon concentration	$2.64 \cdot 10^{-1}$	$2.11 \cdot 10^{-1}$	$3.14 \cdot 10^{-1}$
$X_{38}$	Vegetable respiratory recycling index in fruit vegetable	$1.61 \cdot 10^{-1}$	$1.07 \cdot 10^{-1}$	$2.22 \cdot 10^{-1}$
$X_{43}$	Soil layer solid liquid distribution coefficient for $^{14}\text{C}$	$1.49 \cdot 10^{-1}$	$1.04 \cdot 10^{-1}$	$2.00 \cdot 10^{-1}$
$X_{11}$	Vegetable dry matter fraction in fruit vegetable	$1.37 \cdot 10^{-1}$	$8.34 \cdot 10^{-2}$	$1.93 \cdot 10^{-1}$
$X_3$	Plant daily irrigation rate in fruit vegetable	$7.04 \cdot 10^{-2}$	$3.32 \cdot 10^{-2}$	$1.07 \cdot 10^{-1}$
$X_6$	Fish water content	$5.91 \cdot 10^{-2}$	$3.60 \cdot 10^{-2}$	$8.17 \cdot 10^{-2}$
$X_{16}$	Water infiltration rate	$1.90 \cdot 10^{-2}$	$-7.26 \cdot 10^{-4}$	$4.04 \cdot 10^{-2}$
$X_{42}$	Soil layer clay plus silt fraction	$2.28 \cdot 10^{-3}$	$-2.46 \cdot 10^{-3}$	$7.49 \cdot 10^{-3}$
$X_{15}$	Distribution coefficient for sandy soil and Ag	$-1.97 \cdot 10^{-3}$	$-4.92 \cdot 10^{-3}$	$8.18 \cdot 10^{-4}$
$X_{12}$	Vegetable dry matter fraction in leafy vegetable	$-1.38 \cdot 10^{-3}$	$-3.81 \cdot 10^{-3}$	$1.16 \cdot 10^{-3}$
$X_7$	Reference coefficient partition in matter	$-9.25 \cdot 10^{-4}$	$-2.92 \cdot 10^{-3}$	$1.31 \cdot 10^{-3}$
$X_{13}$	Vegetable dry matter fraction in root vegetable	$8.71 \cdot 10^{-4}$	$-1.53 \cdot 10^{-3}$	$3.28 \cdot 10^{-3}$
$X_{29}$	Vegetable isotopic discrimination for H.3 in fruit vegetable	$-7.35 \cdot 10^{-4}$	$-2.83 \cdot 10^{-3}$	$1.52 \cdot 10^{-3}$
$X_4$	Plant daily irrigation rate in leafy vegetable	$6.32 \cdot 10^{-4}$	$-1.91 \cdot 10^{-3}$	$3.20 \cdot 10^{-3}$
$X_5$	Plant daily irrigation rate in root vegetable	$-3.71 \cdot 10^{-4}$	$-2.46 \cdot 10^{-3}$	$1.81 \cdot 10^{-3}$